NASA-RP-1166 19860018363

NASA Reference Publication 1166

July 1986

Airborne Lidar Measurements of El Chichon Stratospheric Aerosols

July 1982

M. Patrick McCormick
and M. T. Osborn

LIBRARY COPY

LANGLEY RESEARCH CENTER
LIBRARY, NASA
HAMPTON, VIRGINIA

NASA

NASA Reference Publication 1166

1986

Airborne Lidar Measurements of El Chichon Stratospheric Aerosols

July 1982

M. Patrick McCormick
Langley Research Center
Hampton, Virginia

M. T. Osborn
SASC Technologies, Inc.
Hampton, Virginia

National Aeronautics and Space Administration

Scientific and Technical Information Branch

Preface

This is the third in a series of reports presenting results from five extensive lidar flight missions. One of the primary purposes of these missions was to determine the spatial distribution and aerosol characteristics of the El Chichon–produced stratospheric material. This particular mission was chronologically the first and covered 42°N to 12°N in July 1982. Results from the October to November 1982 mission, which covered 46°N to 46°S, were reported by McCormick and Osborn in NASA Reference Publication 1136 entitled "Airborne Lidar Measurements of El Chichon Stratospheric Aerosols—October 1982 to November 1982." Results from the January to February 1983 mission, which covered 27°N to 76°N, were reported by McCormick and Osborn in NASA Reference Publication 1148 entitled "Airborne Lidar Measurements of El Chichon Stratospheric Aerosols—January 1983 to February 1983." The remaining two missions took place in May 1983 and January 1984 and covered the latitudes 72°N to 56°S and 38°N to 90°N, respectively.

This report contains representative profiles of lidar backscatter ratio, plots of integrated backscattering values versus latitude, and contours of backscatter mixing ratio versus altitude and latitude. In addition, tables containing numerical values of the backscatter ratio and backscattering function versus altitude are supplied for each profile. Although no attempt has been made to provide any scientific analysis with the data, this report is intended to give the results of the mission in a ready-to-use format.

The authors recognize the airborne lidar team of W. H. Fuller, Jr., and B. R. Rouse of the NASA Langley Research Center and W. H. Hunt and F. C. Diehl of Wyle Laboratories, whose dedicated efforts provided these data, and wish to thank the crew and supporting personnel at the NASA Wallops Flight Facility for providing an excellent research airplane platform for conducting these measurements. Finally, the authors wish to express their appreciation to D. J. Hofmann and his group at the University of Wyoming for providing the dustsonde data.

Contents

Preface iii

Summary 1

Introduction 1

Airborne Lidar System 1

Flight Path 1

Lidar Profiles 1

Integrated Backscattering 2

Contours of Backscatter Mixing Ratio 2

Optical Depth and Mass 2

Concluding Remarks 2

Figures:

1. Flight path 3
2–25. Lidar scattering-ratio profiles 4
26. Integrated aerosol backscattering function versus latitude 16
27. Averaged integrated backscattering function versus latitude 17
28. Contours of backscatter mixing ratio 18

Appendix—Flight Log and Numerical Values of Scattering Ratios and Scattering Functions for Flight Mission 19

Table A1. Flight Log During Lidar Operation 19

Table A2.–A25. Lidar Scattering Ratio and Scattering Function Versus Altitude for Each Profile 20

References 44

Summary

This report presents lidar data from a flight mission in July 1982 between 42°N and 12°N. The primary purpose of this mission was to determine the spatial distribution and aerosol characteristics of the El Chichon–produced stratospheric material a short time after the March–early April 1982 eruptions. Representative profiles of lidar backscatter ratio, plots of integrated backscattering values versus latitude, and contours of backscattering mixing ratio versus altitude and latitude are presented. In addition, tables containing numerical values of the backscatter ratio and the backscattering function versus altitude are supplied for each profile.

The most massive portion of the material produced by the El Chichon eruptions that was measured by this flight resided south of 30°N and was concentrated above 21 km in a layer that peaked at 24 to 27 km. In this latitude region, peak backscatter ratios at a wavelength of 0.6943 μm were approximately 50, and peak optical depths were calculated to be 0.2. Material below 21 km was less massive but moved to the poles much more rapidly. Some material, for example, reached the Arctic region by late April. No attempt has been made in this report to give any detailed explanations or interpretations of the data. The report provides, in a ready-to-use format, the results of this mission to be used in atmospheric and climatic studies.

Introduction

The late March–early April 1982 eruptions of El Chichon in Mexico (17.3°N, 93.2°W) produced the largest enhancements of stratospheric aerosols in at least 20 years. Because of the effects of the eruption cloud from El Chichon and the need for characterizing the cloud spatially, an experimental survey flight was carried out in July 1982 to map its latitudinal and vertical distributions. A NASA Electra airplane outfitted with a lidar system was flown during the period July 9–12, 1982, between the latitudes of 42°N (upstate New York) and 12°N (off the northern coast of Venezuela).

This report presents the results of the lidar stratospheric measurements taken over the entire mission. Some of the results of this mission were previously published by Labitzke et al. (ref. 1) to show the relationship between an increase in stratospheric temperatures and increased aerosol loading.

Airborne Lidar System

The airborne lidar system used for the measurements presented in this report consists of a ruby laser, nominally emitting 1 joule per pulse at 1 pulse per 2 seconds at a wavelength (λ) of 0.6943 μm during flight, and a 35.6-cm cassegrainian-configured receiving telescope. Two photomultipliers, electronically switched on at specific times after laser firing, are used to enhance dynamic range. The photomultiplier output signals are processed with an analog-to-digital converter and microprocessor computer, stored on magnetic tape, and displayed on an interactive terminal. The transmitted output divergence is 1.0 mrad, and the receiver field-of-view is 2.0 mrad. Two 40.6-cm quartz windows separated by 1 m are used in the top of the fuselage of the airplane. One window is used for the laser transmitter, and the other, for the telescope receiver. The signal becomes usable at 3 to 4 km above the altitude of the airplane. A detailed error analysis for this system is described in Russell et al. (ref. 2).

Flight Path

The flight path for the July 1982 mission is given in figure 1. The northbound and southbound flight legs are represented by solid lines and dashed lines, respectively.

As expected, overlying upper tropospheric clouds prevented measurements at some latitudes, but most latitudes were covered, and a remarkable amount of high-quality data were successfully recorded. Table A1 (in the appendix) contains an abbreviated flight log for the mission and lists the date, time, location, and flight altitude for those legs of the mission where good quality lidar data were obtained.

Lidar Profiles

The lidar backscatter ratio (or scattering ratio) is defined as

$$R(z) = 1 + \frac{f_A(z)}{f_M(z)} \tag{1}$$

where f_A is the aerosol backscattering function, or scattering function, and f_M is the molecular backscattering function, both in units of $(\text{km-sr})^{-1}$ and both at altitude z (ref. 3). Representative vertical profiles of lidar scattering ratio for the flight survey are shown in figures 2 to 25. The tropopause height is indicated by an arrow. Tables A2 to A25 (in the appendix) contain numerical values of the aerosol scattering ratio and scattering function versus altitude for each of these profiles.

These profiles actually underestimate the scattering ratio (and scattering function) by up to 10 percent. The transmission model used in obtaining $R(z)$ from the lidar measurement was based on background aerosol conditions. Later lidar flights used the lidar data to iteratively update the model to reflect the actual aerosol conditions.

The scattering-ratio profiles, reported at 0.30-km intervals, have been smoothed over 0.45 km. The profiles were then normalized to 1, a value which would be obtained only if no aerosols were present at some altitude within the normalization region. Occasionally, the numerical values of the scattering ratio are less than 1, and the corresponding scattering functions are negative. This occurs when the profile contains minima outside the normalization region. Minimum values of the scattering ratio and scattering function should be considered 1 and 0, respectively.

As shown in figures 2 through 25, the bulk of the material produced by the El Chichon eruptions resided south of 30°N and was concentrated above 21 km in a layer that peaked at 24 to 27 km. In the latitude region south of 30°N which was covered by this flight, peak scattering ratios at $\lambda = 0.6943$ μm were approximately 50.

Integrated Backscattering

The integrated aerosol backscattering function is defined as

$$\int_{h_T}^{28\text{ km}} f_A(z)\,dz \qquad (2)$$

where f_A is the aerosol backscattering function $(\text{km-sr})^{-1}$ at altitude z, and h_T is the height of the tropopause at the location where the lidar data were taken. The integrated aerosol backscattering function for all usable lidar data from the July 1982 mission is plotted in figure 26. The solid lines represent values computed from profiles taken on the northbound flight, and the dashed lines represent values computed from profiles taken on the southbound flight. The northbound and southbound data, combined and averaged into 2.5° latitude bins, are shown in figure 27. A small correction to compensate for the use of a background transmission model (see "Lidar Profiles") has been applied to the integrated aerosol backscattering values plotted in figures 26 and 27.

Contours of Backscatter Mixing Ratio

The backscatter mixing ratio is defined as f_A/f_M, or $R(z)-1$. The symbol $R(z)$ was defined previously in equation (1). Contours of backscatter mixing ratio were plotted for all the southbound and northbound lidar data to determine the vertical as well as the latitudinal distribution of the El Chichon–produced aerosol. Figure 28 contains both the northbound and southbound contours. These contours clearly show a ledge in the backscatter mixing ratio at about 30°N. The bulk of the material produced by the El Chichon eruptions of late March–early April 1982 is shown to reside above 21 km. Material below 21 km was less massive but moved to the poles much more rapidly. Some material, for example, reached the Arctic region by late April (ref. 4).

Optical Depth and Mass

An aerosol optical model for the July 1982 flight was constructed by using a six-channel dustsonde launch by the University of Wyoming at 27.8°N (Texas) on August 21, 1982 (ref. 5). The model gives a conversion value from integrated backscattering to column density of 18.3 g-sr/m^2 (ref. 6).

Similarly, using the aerosol characteristics determined from the dustsonde flight as representative of the aerosol over the most massive part of the stratospheric cloud gave a value of 42.5 sr for converting integrated backscattering to optical depth. Peak optical depth values of about 0.2 at $\lambda = 0.6943$ μm were determined at approximately 20°N.

Concluding Remarks

This report has presented a summary of the lidar data obtained during the July 1982 flight mission, which was conducted to determine the spatial distribution and aerosol characteristics of the El Chichon–produced stratospheric material. Vertical profiles of aerosol backscatter ratio were determined over the latitudes of the flight (42°N to 12°N). The most massive portion of the material produced by the El Chichon eruptions of late March–early April 1982 which was measured by this flight resided south of the 30°N and was concentrated above 21 km in a layer that peaked at 24 to 27 km. In this latitude region, peak backscatter ratios at a wavelength of 0.6943 μm were approximately 50, and peak optical depths were calculated to be 0.2. Plots of integrated backscattering values versus latitude and contours of backscatter mixing ratio versus altitude and latitude further describe the latitudinal and vertical distribution of the El Chichon aerosol. In addition, tables containing numerical values of the backscatter ratio and backscattering function versus altitude have been supplied for each profile. Thus, the lidar data from the mission have been presented in a ready-to-use format for further scientific analysis.

NASA Langley Research Center
Hampton, VA 23665-5225
April 21, 1986

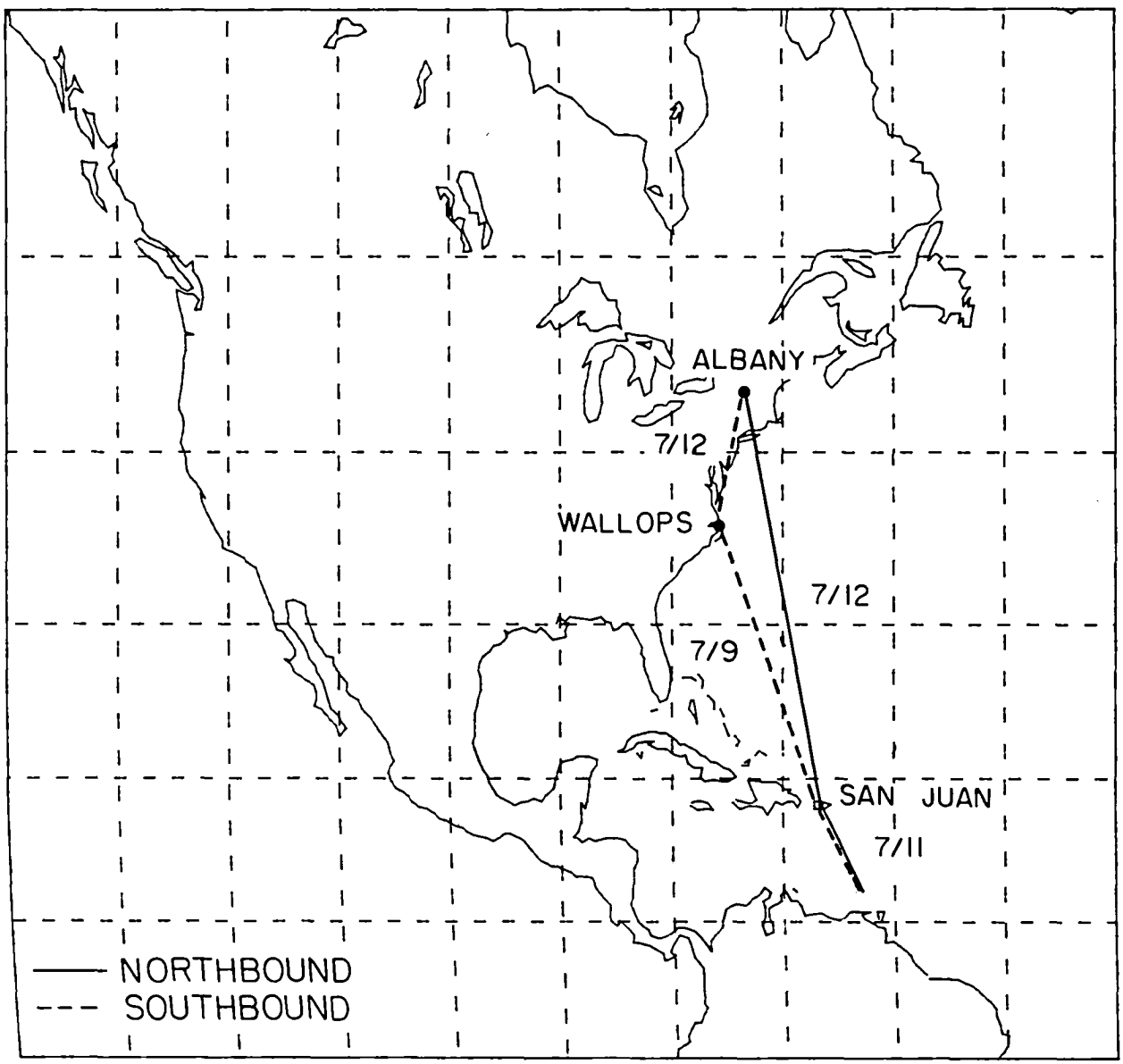

Figure 1. Flight path of NASA Electra airplane from July 9–12, 1982.

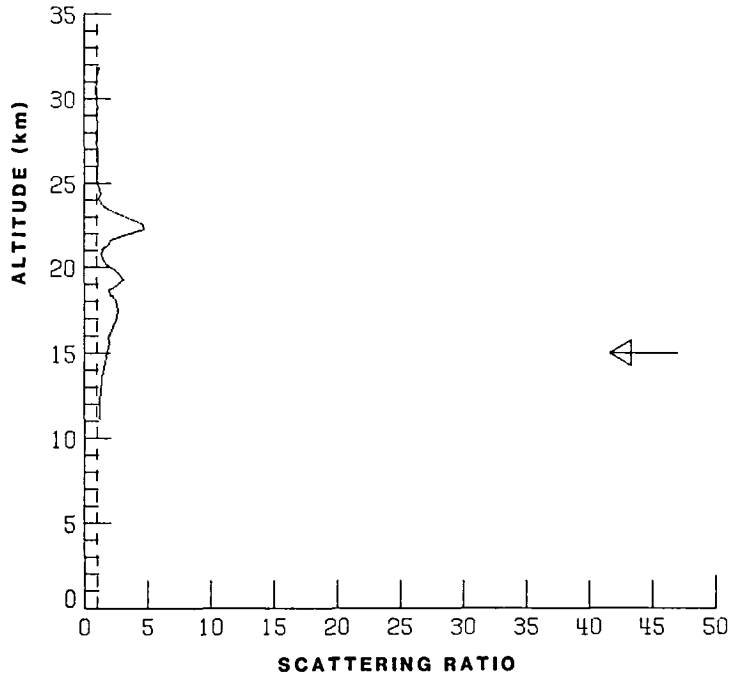

Figure 2. Lidar scattering-ratio profile taken on July 9, 1982, beginning at 35.0°N, 75.0°W at GMT (Greenwich mean time) 0214.

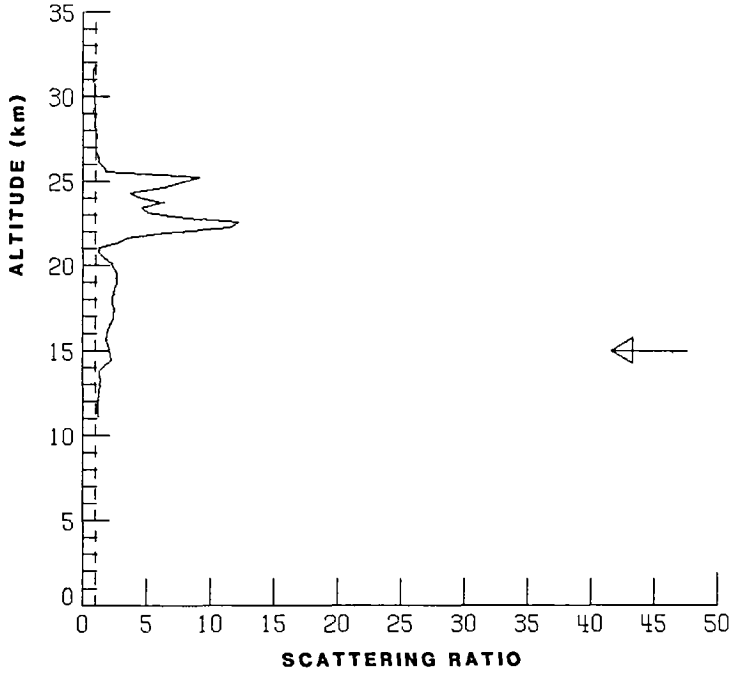

Figure 3. Lidar scattering-ratio profile taken on July 9, 1982, beginning at 32.5°N, 72.5°W at GMT 0256.

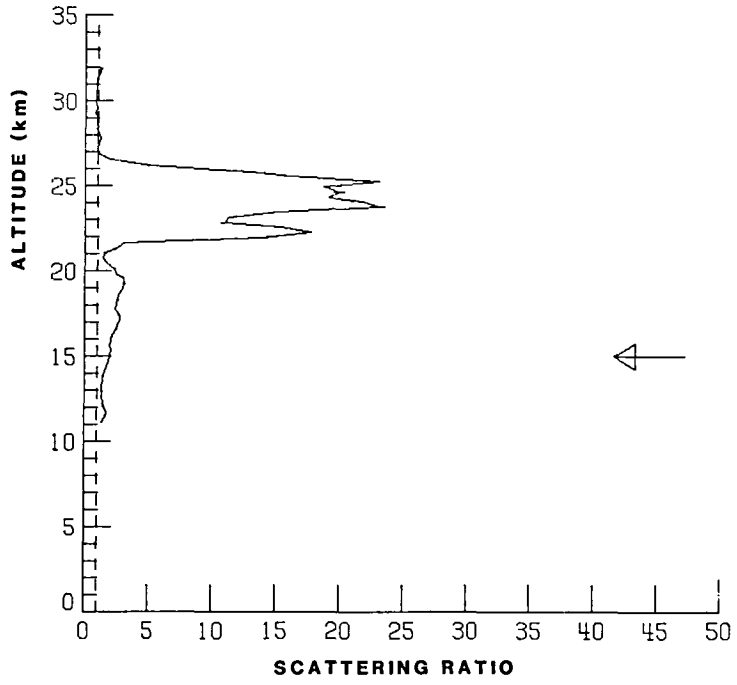

Figure 4. Lidar scattering-ratio profile taken on July 9, 1982, beginning at 31.0°N, 71.5°W at GMT 0314.

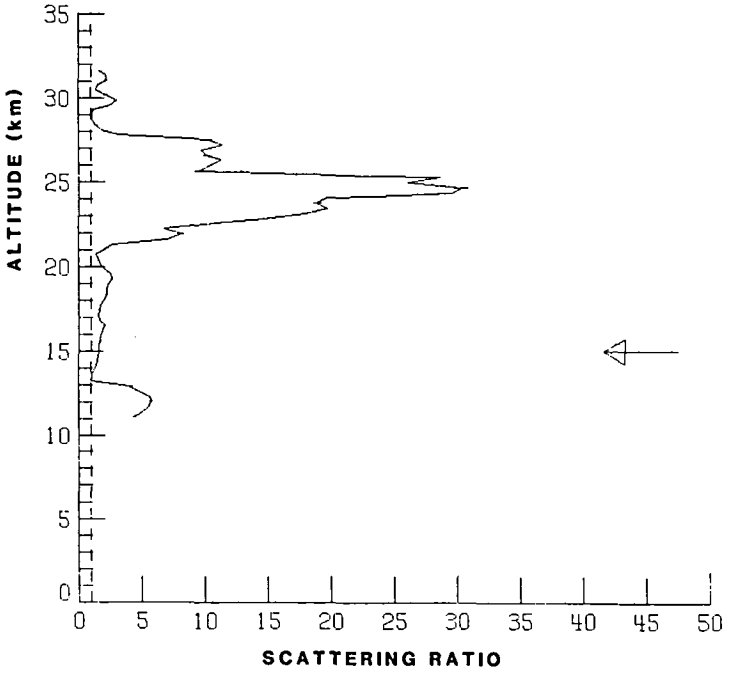

Figure 5. Lidar scattering-ratio profile taken on July 9, 1982, beginning at 29.0°N, 70.0°W at GMT 0353.

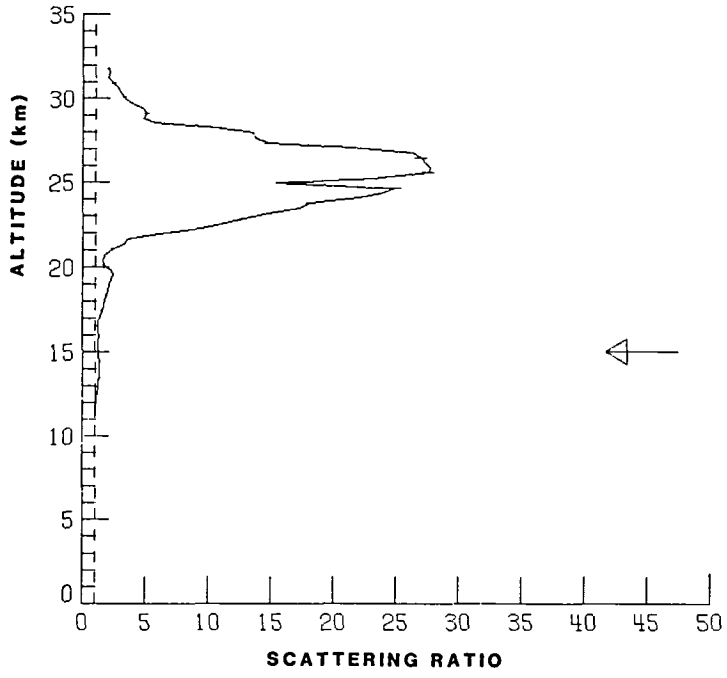

Figure 6. Lidar scattering-ratio profile taken on July 9, 1982, beginning at 26.0°N, 68.5°W at GMT 0415.

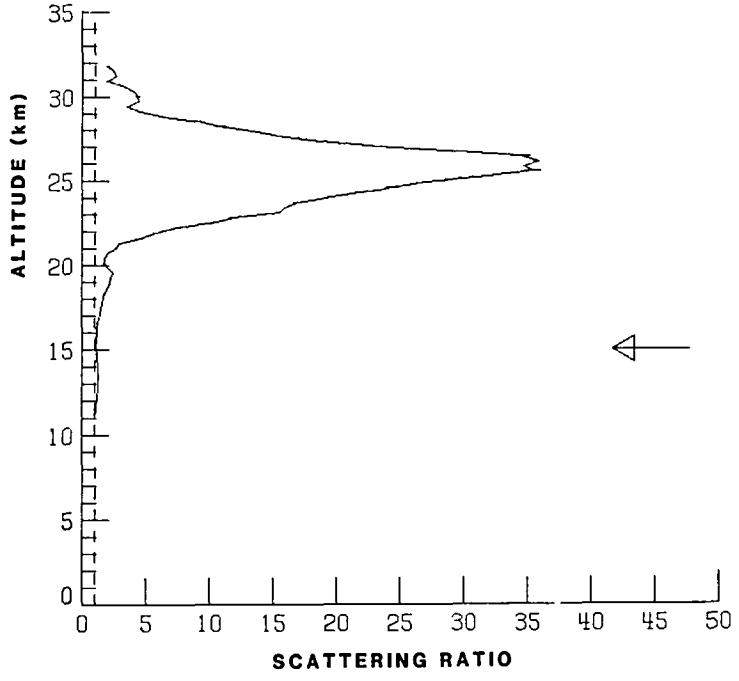

Figure 7. Lidar scattering-ratio profile taken on July 9, 1982, beginning at 24.5°N, 68.0°W at GMT 0444.

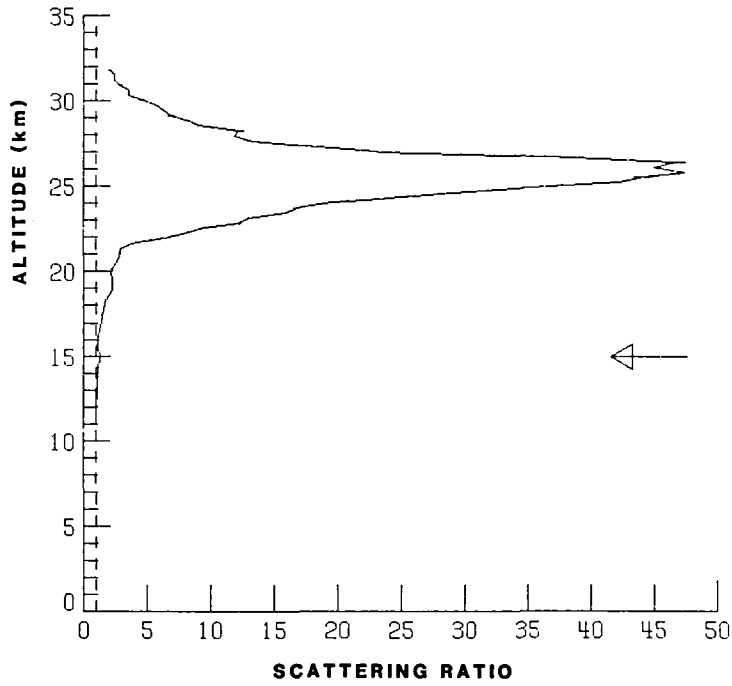

Figure 8. Lidar scattering-ratio profile taken on July 9, 1982, beginning at 22.0°N, 67.5°W at GMT 0508.

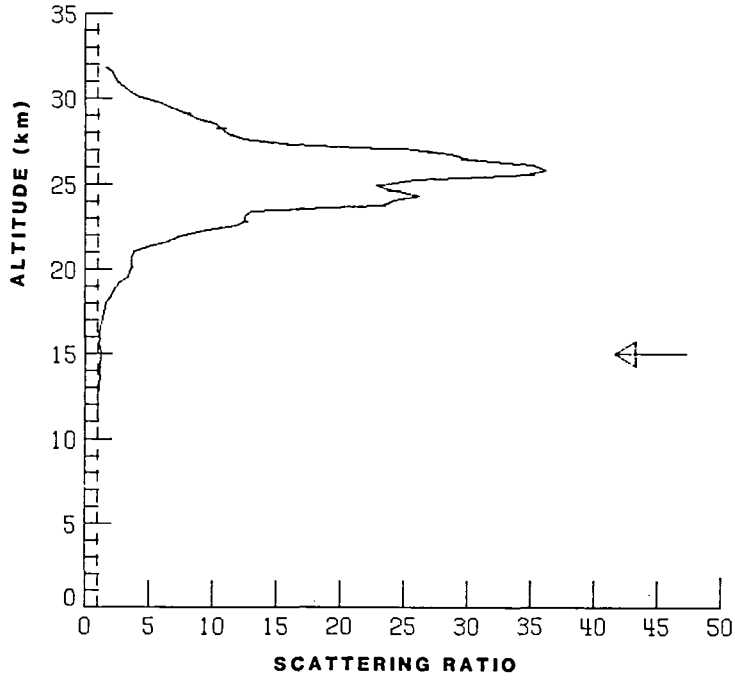

Figure 9. Lidar scattering-ratio profile taken on July 9, 1982, beginning at 20.0°N, 67.0°W at GMT 0531.

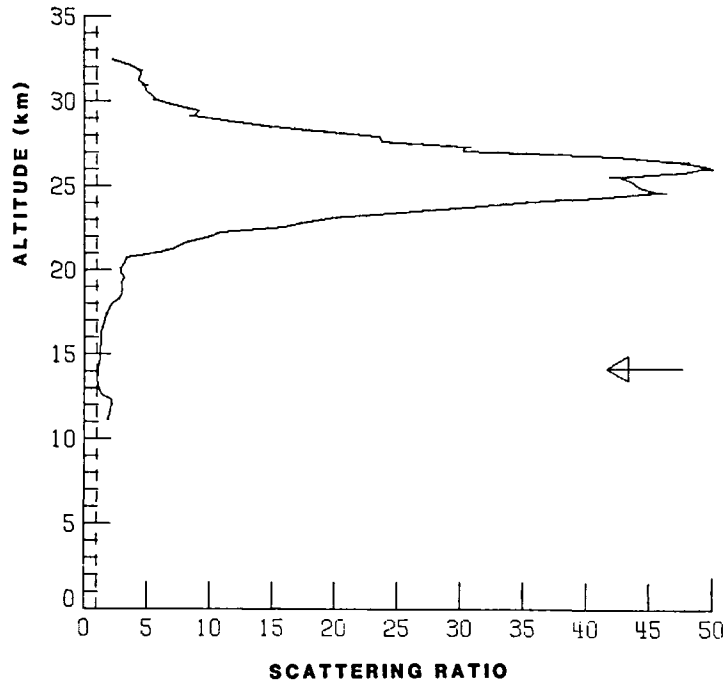

Figure 10. Lidar scattering-ratio profile taken on July 11, 1982, beginning at 17.5°N, 64.5°W at GMT 0216.

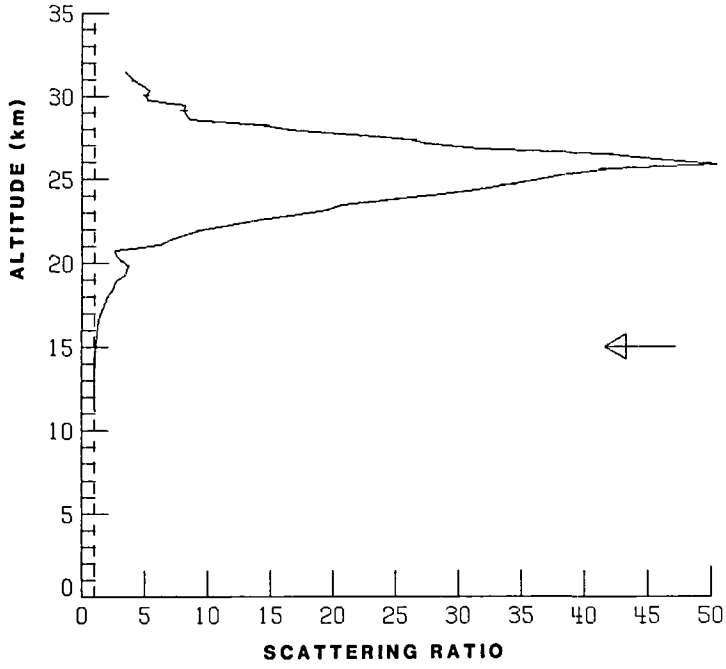

Figure 11. Lidar scattering-ratio profile taken on July 11, 1982, beginning at 16.5°N, 63.0°W at GMT 0238.

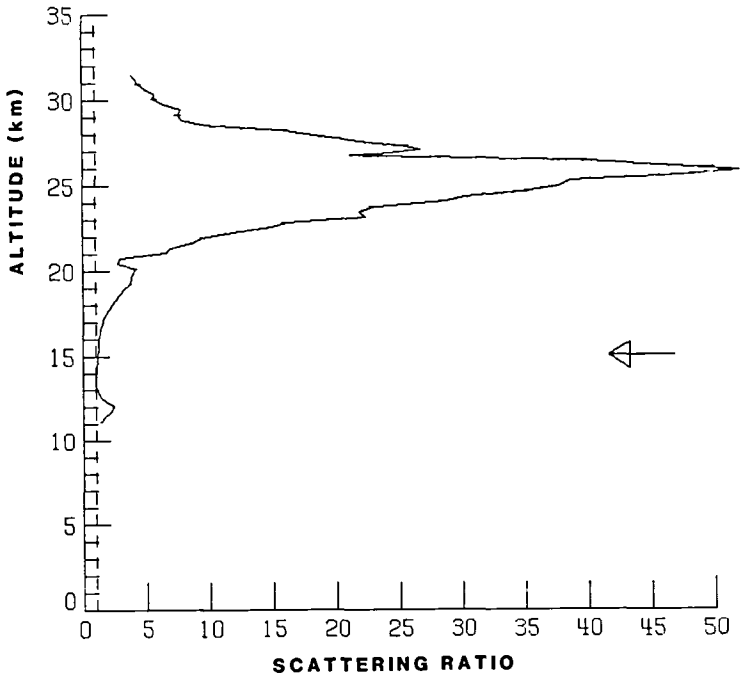

Figure 12. Lidar scattering-ratio profile taken on July 11, 1982, beginning at 15.8°N, 63.0°W at GMT 0247.

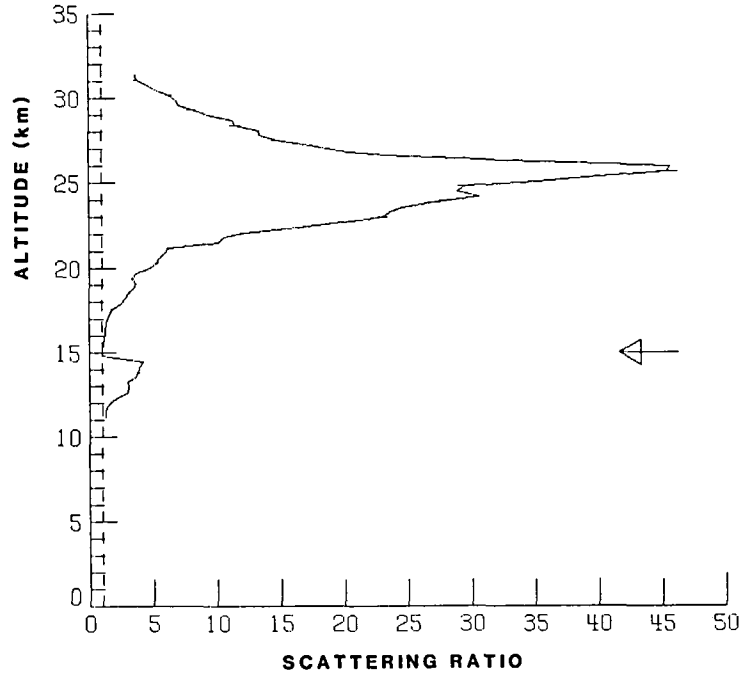

Figure 13. Lidar scattering-ratio profile taken on July 11, 1982, beginning at 13.0°N, 62.8°W at GMT 0320.

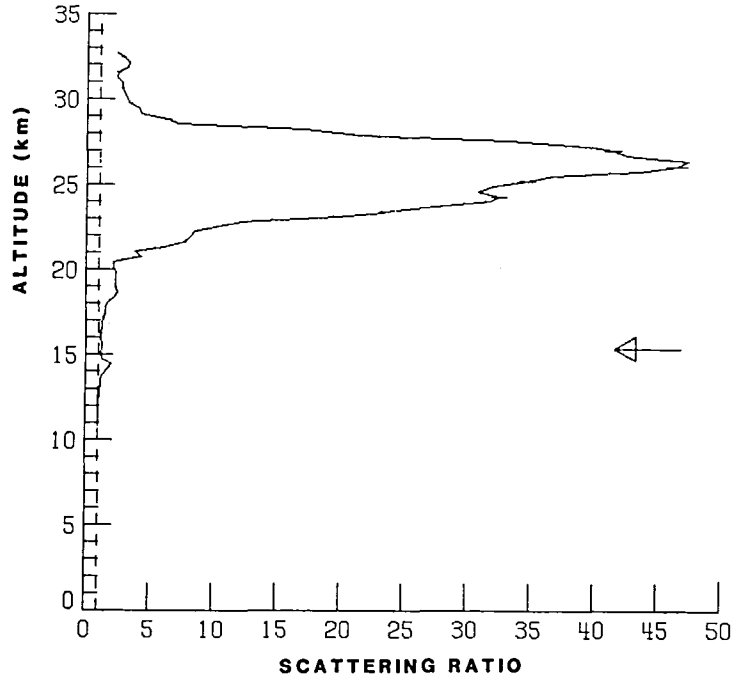

Figure 14. Lidar scattering-ratio profile taken on July 12, 1982, beginning at 21.3°N, 66.8°W at GMT 0016.

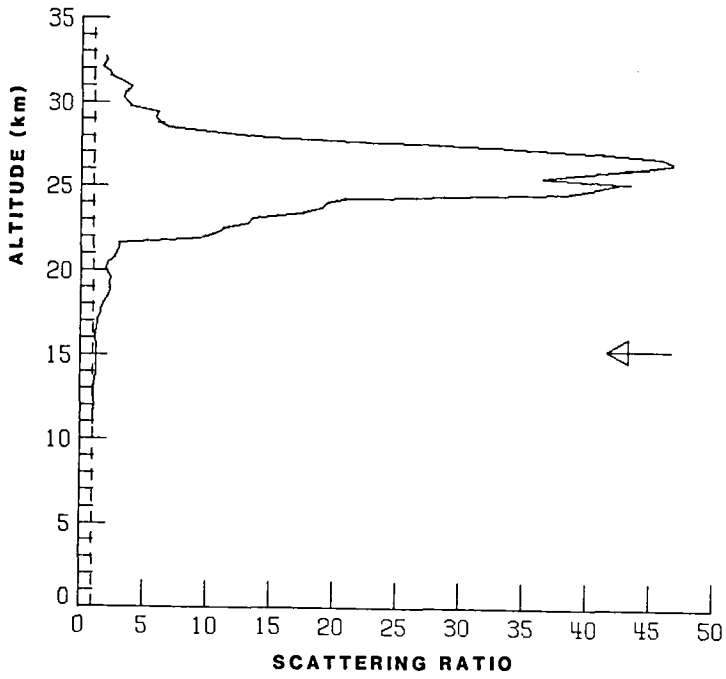

Figure 15. Lidar scattering-ratio profile taken on July 12, 1982, beginning at 23.2°N, 67.4°W at GMT 0042.

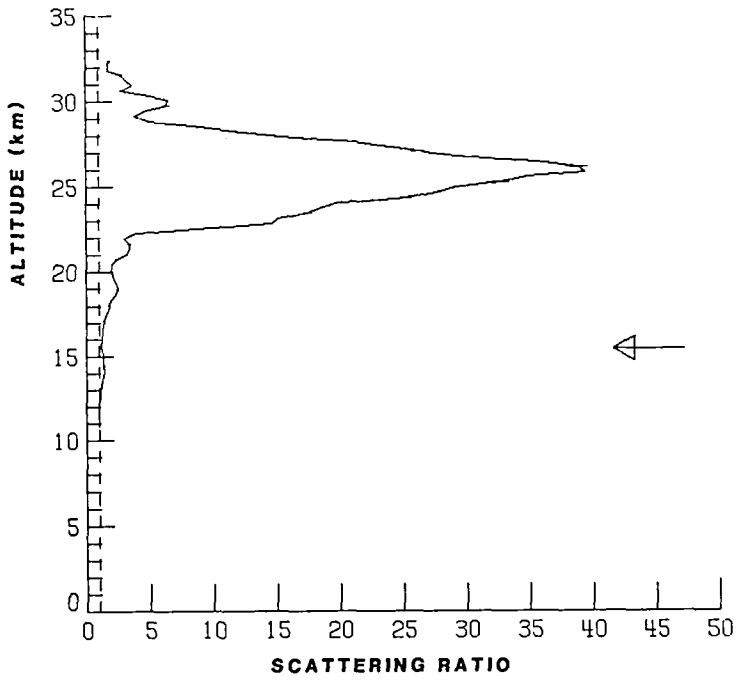

Figure 16. Lidar scattering-ratio profile taken on July 12, 1982, beginning at 24.8°N, 68.0°W at GMT 0102.

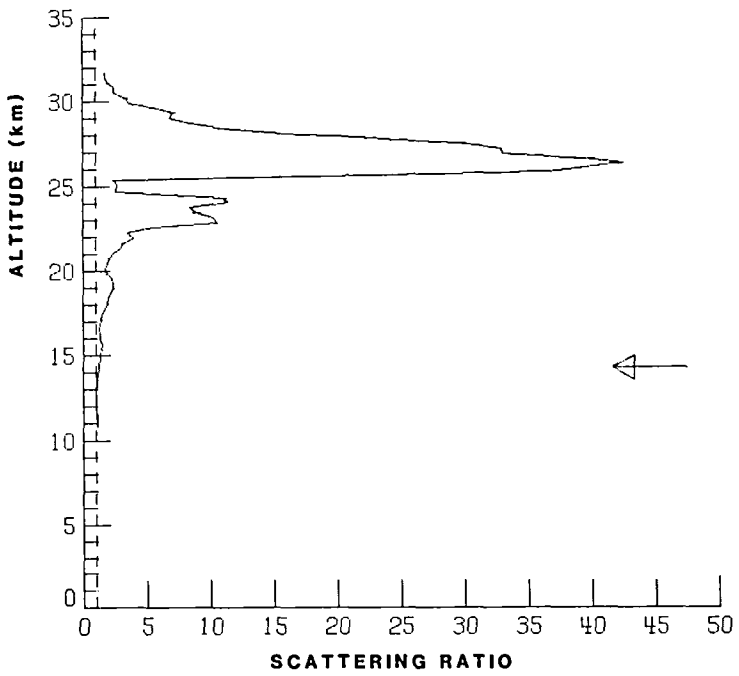

Figure 17. Lidar scattering-ratio profile taken on July 12, 1982, beginning at 27.8°N, 68.8°W at GMT 0143.

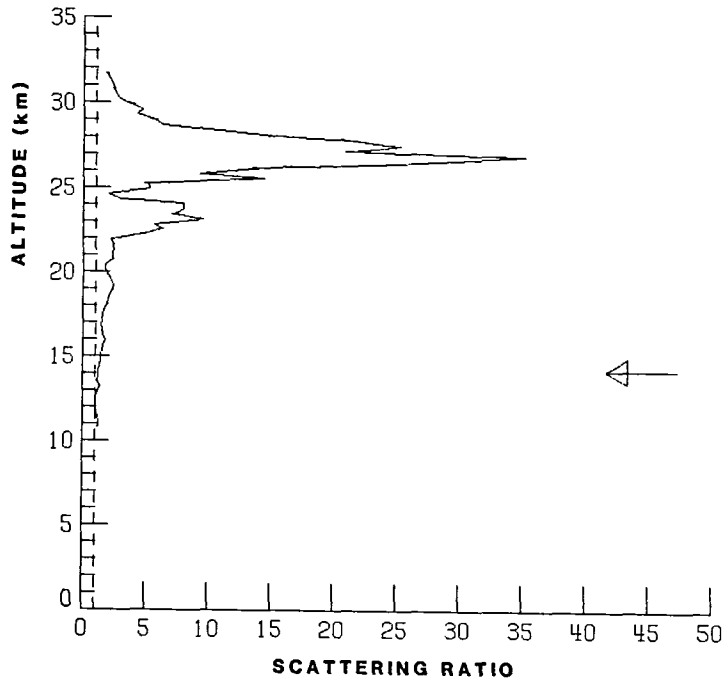

Figure 18. Lidar scattering-ratio profile taken on July 12, 1982, beginning at 29.0°N, 69.2°W at GMT 0158.

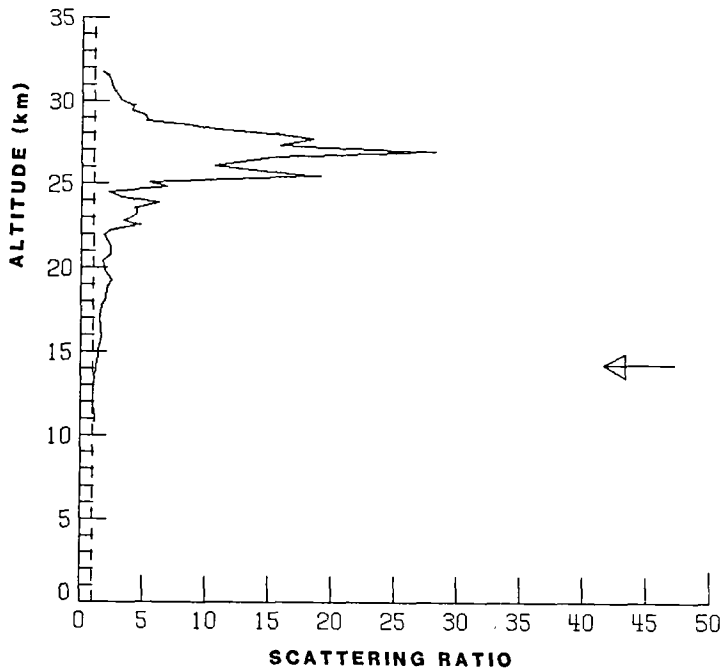

Figure 19. Lidar scattering-ratio profile taken on July 12, 1982, beginning at 29.3°N, 69.3°W at GMT 0202.

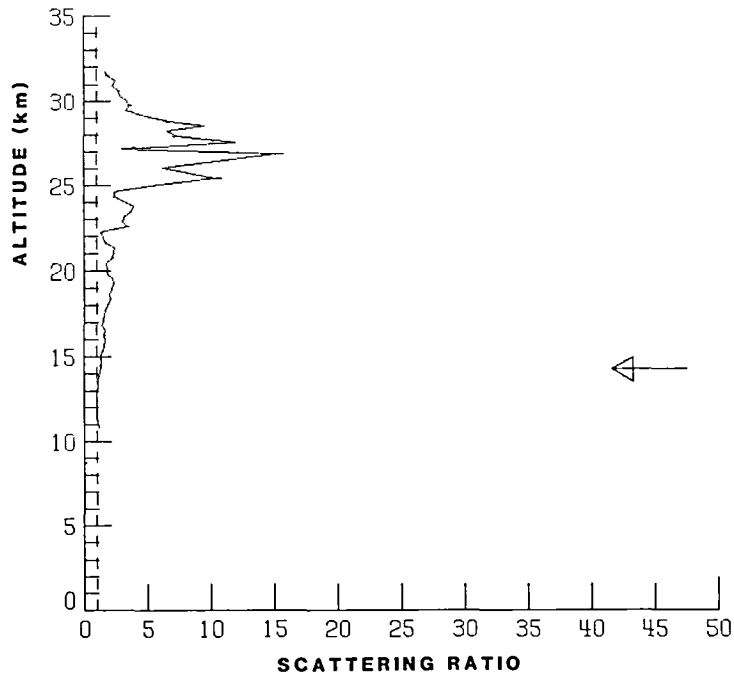

Figure 20. Lidar scattering-ratio profile taken on July 12, 1982, beginning at 29.5°N, 69.3°W at GMT 0205.

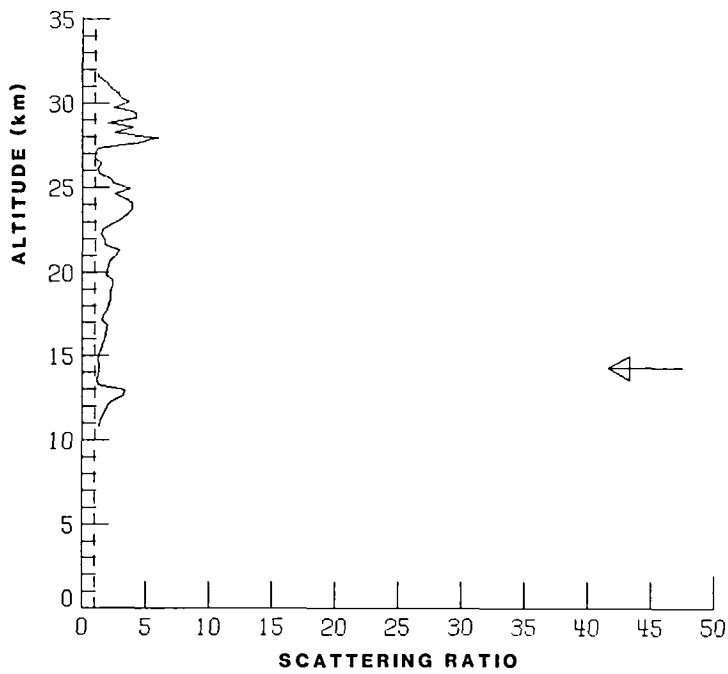

Figure 21. Lidar scattering-ratio profile taken on July 12, 1982, beginning at 30.2°N, 69.6°W at GMT 0213.

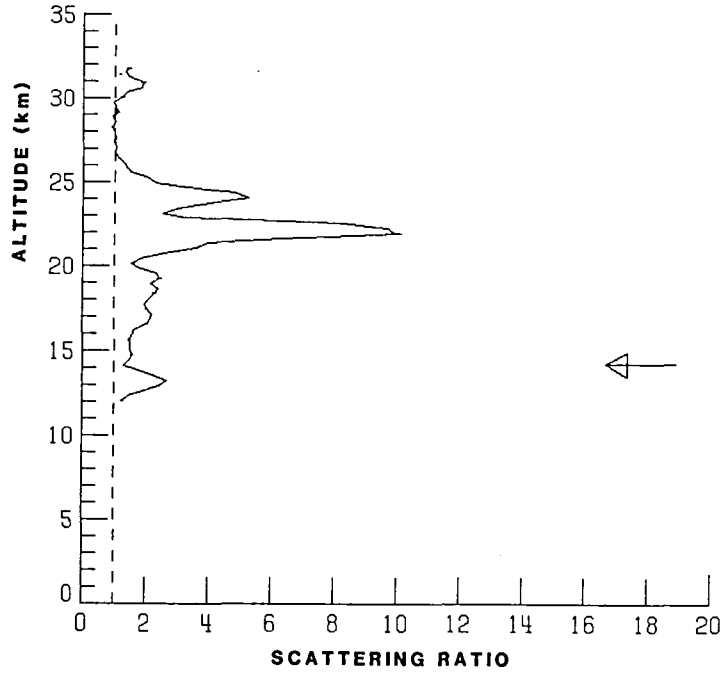

Figure 22. Lidar scattering-ratio profile taken on July 12, 1982, beginning at 32.3°N, 70.1°W at GMT 0238.

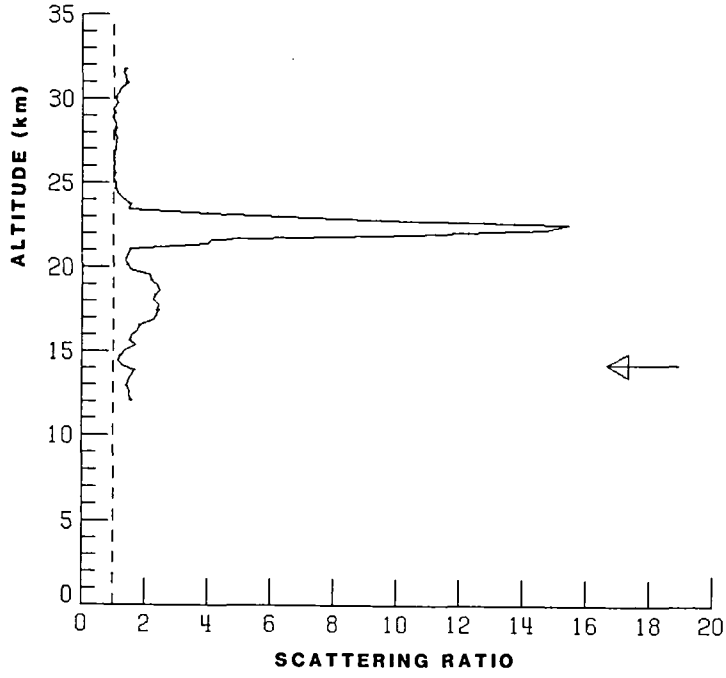

Figure 23. Lidar scattering-ratio profile taken on July 12, 1982, beginning at 34.2°N, 70.7°W at GMT 0306.

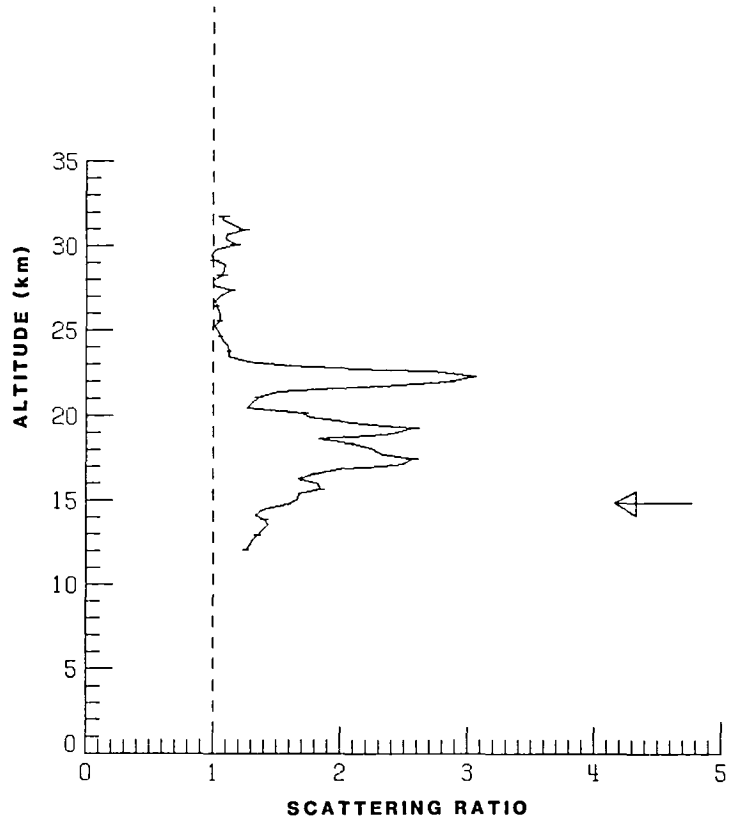

Figure 24. Lidar scattering-ratio profile taken on July 12, 1982, beginning at 38.5°N, 72.0°W at GMT 0403.

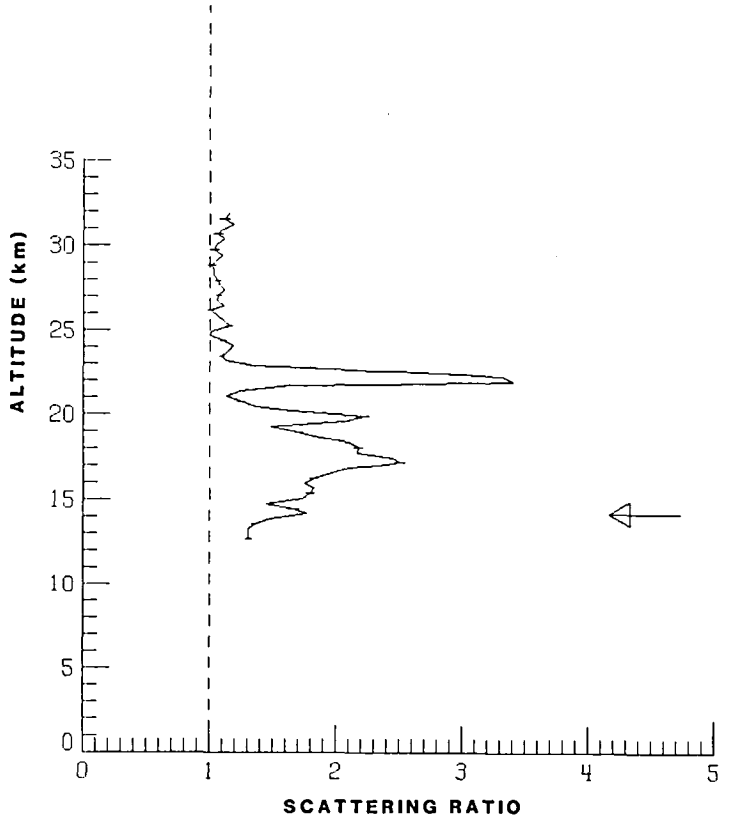

Figure 25. Lidar scattering-ratio profile taken on July 12, 1982, beginning at 42.0°N, 73.7°W at GMT 0506.

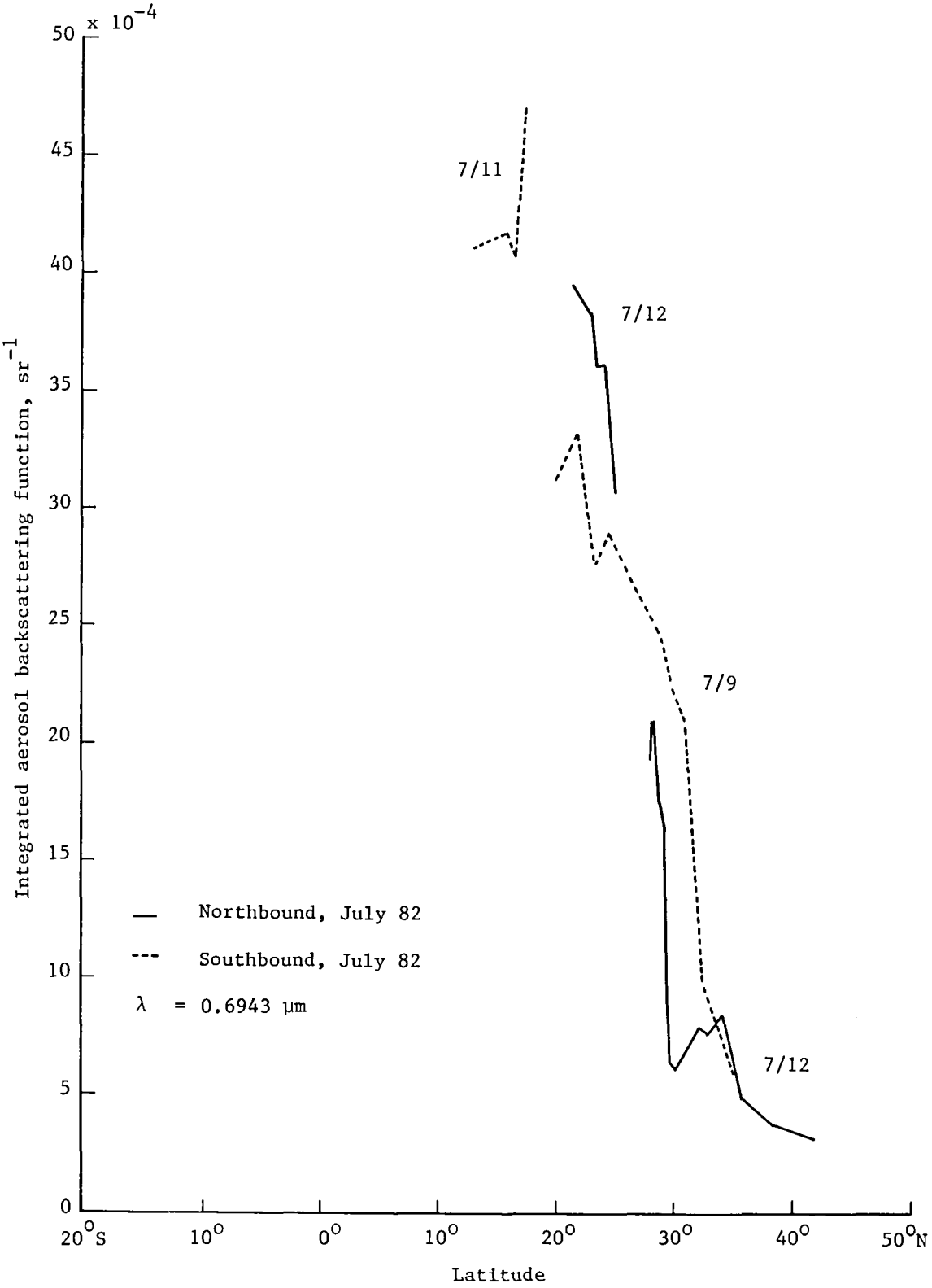

Figure 26. Integrated aerosol backscattering function from the tropopause through the stratospheric layer versus latitude for northbound and southbound flights.

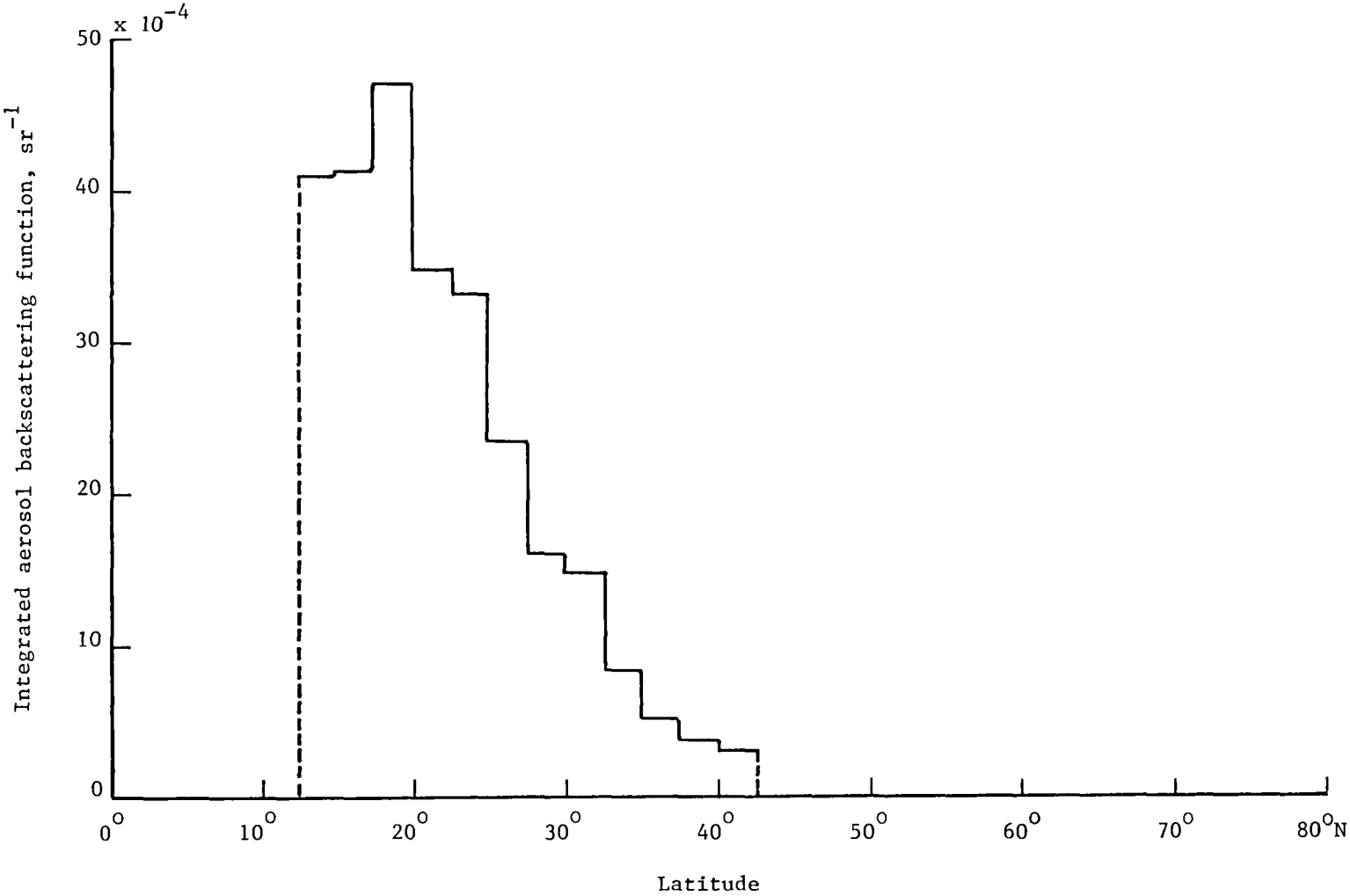

Figure 27. Integrated aerosol backscattering function averaged into 2.5° latitude bins (calculated from data in fig. 26).

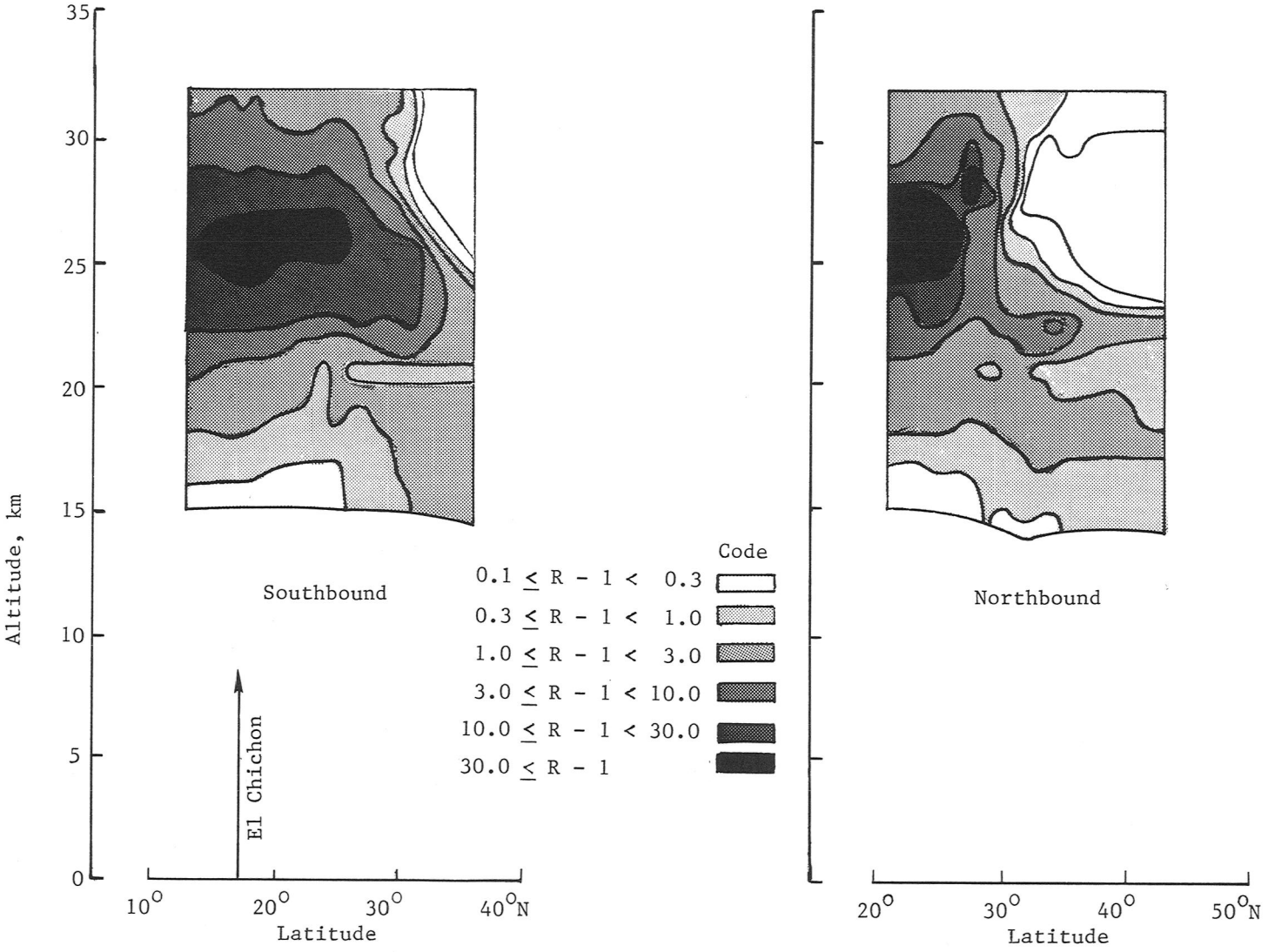

Figure 28. Contours of backscatter mixing ratio for data collected during southbound and northbound flight legs.

Appendix

Flight Log and Numerical Values for Scattering Ratios and Scattering Functions for Flight Mission

TABLE A1. FLIGHT LOG DURING LIDAR OPERATION

Date	GMT[a]	Location	Altitude, ft
July 9	0214–0551	35.8°N, 75.5°W–19.6°N, 66.5°W	21 000
July 11	0216–0332	18.0°N, 64.8°W–12.7°N, 62.6°W	21 000
July 12	0016–0108	21.1°N, 66.7°W–25.0°N, 68.0°W	20 000
	0143–0221	27.7°N, 68.8°W–30.6°N, 69.7°W	20 000
	0238–0414	31.8°N, 70.0°W–39.0°N, 72.0°W	24 000
	0447–0502	41.5°N, 73.7°W–42.5°N, 73.7°W	24 000
	0506–0521	42.5°N, 73.7°W–41.4°N, 73.7°W	26 000

[a]Greenwich mean time.

TABLE A2. LIDAR DATA TAKEN ON JULY 9, 1982, BEGINNING AT 35.0°N, 75.0°W AT GMT (GREENWICH MEAN TIME) 0214

Altitude, km	Scattering ratio	Scattering function, $(km\text{-}sr)^{-1}$	Altitude, km	Scattering ratio	Scattering function, $(km\text{-}sr)^{-1}$
11.139	1.178	.2884E-04	22.839	3.874	.7454E-04
11.439	1.169	.2653E-04	23.139	2.868	.4619E-04
11.739	1.162	.2446E-04	23.439	1.945	.2228E-04
12.039	1.173	.2516E-04	23.739	1.395	.8875E-05
12.339	1.179	.2517E-04	24.039	1.195	.4177E-05
12.639	1.209	.2824E-04	24.339	1.318	.6508E-05
12.939	1.230	.2997E-04	24.639	1.208	.4061E-05
13.239	1.263	.3287E-04	24.939	1.084	.1560E-05
13.539	1.345	.4149E-04	25.239	1.000	0.
13.839	1.382	.4413E-04	25.539	1.036	.6116E-06
14.139	1.491	.5459E-04	25.839	1.031	.5004E-06
14.439	1.532	.5647E-04	26.139	1.072	.1101E-05
14.739	1.628	.6337E-04	26.439	1.050	.7387E-06
15.039	1.715	.6866E-04	26.739	1.044	.6106E-06
15.339	1.747	.6819E-04	27.039	1.032	.4330E-06
15.639	1.778	.6756E-04	27.339	1.015	.1960E-06
15.939	1.724	.5980E-04	27.639	1.091	.1100E-05
16.239	1.910	.7148E-04	27.939	1.121	.1400E-05
16.539	2.131	.8452E-04	28.239	1.090	.9897E-06
16.839	2.244	.8827E-04	28.539	1.064	.6747E-06
17.139	2.305	.8784E-04	28.839	1.005	.4711E-07
17.439	2.436	.9175E-04	29.139	1.026	.2510E-06
17.739	2.328	.8048E-04	29.439	1.053	.4888E-06
18.039	2.246	.7165E-04	29.739	1.008	.7112E-07
18.339	1.944	.5148E-04	30.039	1.012	.1013E-06
18.639	1.774	.4007E-04	30.339	.962	-.3009E-06
18.939	2.265	.6211E-04	30.639	.937	-.4774E-06
19.239	2.839	.8589E-04	30.939	.977	-.1688E-06
19.539	2.674	.7432E-04	31.239	.992	-.5415E-07
19.839	2.301	.5493E-04	31.539	1.102	.6735E-06
20.139	1.746	.2994E-04	31.764	1.192	.1228E-05
20.439	1.406	.1550E-04			
20.739	1.263	.9531E-05			
21.039	1.412	.1423E-04			
21.339	1.716	.2358E-04			
21.639	2.172	.3677E-04			
21.939	3.272	.6799E-04			
22.239	4.702	.1056E-03			
22.539	4.637	.9895E-04			

TABLE A3. LIDAR DATA TAKEN ON JULY 9, 1982, BEGINNING AT 32.5°N, 72.5°W AT GMT 0256

Altitude, km	Scattering ratio	Scattering function, $(km\text{-}sr)^{-1}$	Altitude, km	Scattering ratio	Scattering function, $(km\text{-}sr)^{-1}$
11.139	1.079	.1284E-04	22.839	7.946	.1802E-03
11.439	1.079	.1240E-04	23.139	5.055	.1003E-03
11.739	1.082	.1247E-04	23.439	4.589	.8464E-04
12.039	1.072	.1049E-04	23.739	6.079	.1142E-03
12.339	1.082	.1155E-04	24.039	4.279	.7030E-04
12.639	1.114	.1537E-04	24.339	3.664	.5446E-04
12.939	1.215	.2802E-04	24.639	6.238	.1021E-03
13.239	1.256	.3204E-04	24.939	7.573	.1222E-03
13.539	1.188	.2259E-04	25.239	9.085	.1433E-03
13.839	1.142	.1648E-04	25.539	1.829	.1401E-04
14.139	1.514	.5719E-04	25.839	1.641	.1033E-04
14.439	2.015	.1077E-03	26.139	1.246	.3780E-05
14.739	1.934	.9425E-04	26.439	1.229	.3352E-05
15.039	1.827	.7939E-04	26.739	1.036	.5080E-06
15.339	1.735	.6715E-04	27.039	1.000	0.
15.639	1.642	.5576E-04	27.339	1.012	.1491E-06
15.939	1.642	.5303E-04	27.639	1.078	.9522E-06
16.239	1.761	.5982E-04	27.939	1.013	.1510E-06
16.539	2.007	.7526E-04	28.239	.952	-.5292E-06
16.839	2.117	.7928E-04	28.539	.958	-.4382E-06
17.139	2.122	.7555E-04	28.839	.959	-.4100E-06
17.439	2.180	.7540E-04	29.139	.928	-.1651E-05
17.739	2.080	.6542E-04	29.439	.966	-.3134E-06
18.039	2.005	.5781E-04	29.739	.924	-.6694E-06
18.339	2.147	.6254E-04	30.039	.922	-.6519E-06
18.639	2.172	.6062E-04	30.339	.912	-.7025E-06
18.939	2.386	.6809E-04	30.639	.945	-.4150E-06
19.239	2.361	.6357E-04	30.939	.873	-.9228E-06
19.539	2.340	.5951E-04	31.239	.826	-.1209E-05
19.839	2.154	.4873E-04	31.539	.859	-.9323E-06
20.139	1.936	.3758E-04	31.764	1.012	.7644E-07
20.439	1.511	.1952E-04			
20.739	1.134	.4862E-05			
21.039	1.311	.1074E-04			
21.339	2.122	.3693E-04			
21.639	3.438	.7650E-04			
21.939	6.199	.1556E-03			
22.239	11.165	.2900E-03			
22.539	11.841	.2949E-03			

TABLE A4. LIDAR DATA TAKEN ON JULY 9, 1982, BEGINNING AT 31.0°N, 71.5°W AT GMT 0314

Altitude, km	Scattering ratio	Scattering function, $(km\text{-}sr)^{-1}$	Altitude, km	Scattering ratio	Scattering function, $(km\text{-}sr)^{-1}$
11.139	1.415	.6744E-04	22.839	10.911	.2571E-03
11.439	1.724	.1135E-03	23.139	11.189	.2520E-03
11.739	1.802	.1212E-03	23.439	15.058	.3315E-03
12.039	1.571	.8321E-04	23.739	22.925	.4929E-03
12.339	1.464	.6529E-04	24.039	21.687	.4435E-03
12.639	1.399	.5401E-04	24.339	18.988	.3677E-03
12.939	1.387	.5030E-04	24.639	19.744	.3653E-03
13.239	1.386	.4828E-04	24.939	18.619	.3275E-03
13.539	1.394	.4736E-04	25.239	22.892	.3880E-03
13.839	1.454	.5252E-04	25.539	15.965	.2529E-03
14.139	1.560	.6228E-04	25.839	12.874	.1914E-03
14.439	1.774	.8212E-04	26.139	6.733	.8811E-04
14.739	1.906	.9140E-04	26.439	2.123	.1646E-04
15.039	2.009	.9686E-04	26.739	1.477	.6663E-05
15.339	2.105	.1009E-03	27.039	1.000	0.
15.639	2.007	.8743E-04	27.339	1.021	.2647E-06
15.939	2.046	.8636E-04	27.639	1.103	.1249E-05
16.239	2.192	.9362E-04	27.939	1.333	.3862E-05
16.539	2.498	.1119E-03	28.239	.995	-.5052E-07
16.839	2.590	.1129E-03	28.539	.972	-.2933E-06
17.139	2.707	.1149E-03	28.839	.893	-.1074E-05
17.439	2.702	.1087E-03	29.139	.852	-.1424E-05
17.739	2.427	.8648E-04	29.439	.888	-.1031E-05
18.039	2.463	.8409E-04	29.739	.885	-.1008E-05
18.339	2.558	.8500E-04	30.039	.751	-.2083E-05
18.639	2.634	.8454E-04	30.339	.841	-.1268E-05
18.939	2.972	.9685E-04	30.639	.871	-.9794E-06
19.239	3.061	.9627E-04	30.939	.912	-.6368E-06
19.539	3.022	.8978E-04	31.239	.924	-.5293E-06
19.839	2.453	.6136E-04	31.539	.906	-.6208E-06
20.139	2.349	.5416E-04	31.764	1.167	.1068E-05
20.439	1.711	.2713E-04			
20.739	1.416	.1510E-04			
21.039	1.541	.1869E-04			
21.339	2.497	.4928E-04			
21.639	2.994	.6258E-04			
21.939	13.691	.3798E-03			
22.239	17.596	.4735E-03			
22.539	15.279	.3884E-03			

TABLE A5. LIDAR DATA TAKEN ON JULY 9, 1982, BEGINNING AT 29.0°N, 70.0°W AT GMT 0353

Altitude, km	Scattering ratio	Scattering function, $(km\text{-}sr)^{-1}$	Altitude, km	Scattering ratio	Scattering function, $(km\text{-}sr)^{-1}$
11.139	4.638	.5910E-03	22.839	14.648	.3540E-03
11.439	5.360	.6832E-03	23.139	17.785	.4151E-03
11.739	5.908	.7417E-03	23.439	19.595	.4385E-03
12.039	6.030	.7331E-03	23.739	18.796	.4001E-03
12.339	5.936	.6939E-03	24.039	19.476	.3961E-03
12.639	4.947	.5341E-03	24.339	29.314	.5787E-03
12.939	4.150	.4098E-03	24.639	30.120	.5676E-03
13.239	1.000	0.	24.939	25.936	.4635E-03
13.539	1.058	.6938E-05	25.239	28.418	.4860E-03
13.839	1.142	.1644E-04	25.539	16.914	.2690E-03
14.139	1.433	.4820E-04	25.839	9.383	.1351E-03
14.439	1.516	.5474E-04	26.139	10.743	.1497E-03
14.739	1.539	.5440E-04	26.439	10.747	.1429E-03
15.039	1.551	.5292E-04	26.739	9.235	.1151E-03
15.339	1.606	.5536E-04	27.039	10.846	.1312E-03
15.639	1.685	.5951E-04	27.339	11.266	.1306E-03
15.939	1.757	.6254E-04	27.639	7.371	.7733E-04
16.239	1.868	.6820E-04	27.939	2.412	.1635E-04
16.539	2.039	.7767E-04	28.239	1.704	.7782E-05
16.839	1.687	.4874E-04	28.539	1.238	.2506E-05
17.139	1.557	.3748E-04	28.839	.992	-.8009E-07
17.439	1.616	.3936E-04	29.139	1.215	.2067E-05
17.739	1.745	.4514E-04	29.439	1.098	.8983E-06
18.039	2.074	.6172E-04	29.739	3.102	.1639E-04
18.339	2.197	.6528E-04	30.039	2.883	.1573E-04
18.639	2.255	.6495E-04	30.339	1.748	.5959E-05
18.939	2.330	.6534E-04	30.639	1.413	.3144E-05
19.239	2.620	.7566E-04	30.939	2.178	.8548E-05
19.539	2.585	.7037E-04	31.239	2.292	.8947E-05
19.839	2.124	.4748E-04	31.539	1.896	.5921E-05
20.139	1.734	.2947E-04	31.764	1.303	.1931E-05
20.439	1.535	.2042E-04			
20.739	1.436	.1584E-04			
21.039	2.128	.3894E-04			
21.339	2.679	.5526E-04			
21.639	7.007	.1885E-03			
21.939	8.083	.2120E-03			
22.239	6.776	.1648E-03			
22.539	10.747	.2652E-03			

TABLE A6. LIDAR DATA TAKEN ON JULY 9, 1982, BEGINNING AT 26.0°N, 68.5°W AT GMT 0415

Altitude, km	Scattering ratio	Scattering function, $(km\text{-}sr)^{-1}$	Altitude, km	Scattering ratio	Scattering function, $(km\text{-}sr)^{-1}$
11.139	1.000	0.	22.839	12.312	.2934E-03
11.439	1.012	.1841E-05	23.139	14.164	.3256E-03
11.739	1.028	.4246E-05	23.439	16.573	.3672E-03
12.039	1.044	.6374E-05	23.739	17.411	.3690E-03
12.339	1.106	.1496E-04	24.039	21.101	.4309E-03
12.639	1.158	.2141E-04	24.339	22.797	.4455E-03
12.939	1.195	.2532E-04	24.639	23.868	.4457E-03
13.239	1.268	.3358E-04	24.939	14.771	.2560E-03
13.539	1.322	.3875E-04	25.239	22.780	.3860E-03
13.839	1.304	.3511E-04	25.539	26.455	.4302E-03
14.139	1.287	.3196E-04	25.839	26.593	.4125E-03
14.439	1.270	.2868E-04	26.139	26.224	.3877E-03
14.739	1.224	.2256E-04	26.439	25.898	.3649E-03
15.039	1.206	.1981E-04	26.739	25.271	.3392E-03
15.339	1.183	.1669E-04	27.039	20.517	.2601E-03
15.639	1.206	.1792E-04	27.339	14.268	.1688E-03
15.939	1.249	.2057E-04	27.639	13.209	.1482E-03
16.239	1.190	.1491E-04	27.939	13.040	.1395E-03
16.539	1.171	.1277E-04	28.239	10.173	.1014E-03
16.839	1.211	.1500E-04	28.539	5.529	.4778E-04
17.139	1.350	.2355E-04	28.839	4.606	.3631E-04
17.439	1.483	.3082E-04	29.139	4.870	.3718E-04
17.739	1.589	.3571E-04	29.439	4.580	.3283E-04
18.039	1.677	.3891E-04	29.739	3.563	.2242E-04
18.339	1.799	.4360E-04	30.039	3.144	.1791E-04
18.639	1.905	.4682E-04	30.339	2.895	.1510E-04
18.939	2.037	.5094E-04	30.639	2.730	.1316E-04
19.239	2.162	.5425E-04	30.939	2.357	.9853E-05
19.539	2.290	.5730E-04	31.239	1.923	.6395E-05
19.839	2.168	.4933E-04	31.539	2.114	.7365E-05
20.139	1.582	.2336E-04	31.764	2.008	.6434E-05
20.439	1.513	.1958E-04			
20.739	1.729	.2648E-04			
21.039	2.282	.4424E-04			
21.339	3.132	.7019E-04			
21.639	3.470	.7750E-04			
21.939	5.768	.1427E-03			
22.239	9.033	.2292E-03			
22.539	10.859	.2682E-03			

TABLE A7. LIDAR DATA TAKEN ON JULY 9, 1982, BEGINNING AT 24.5°N, 68.0°W AT GMT 0444

Altitude, km	Scattering ratio	Scattering function, $(km\text{-}sr)^{-1}$	Altitude, km	Scattering ratio	Scattering function, $(km\text{-}sr)^{-1}$
11.139	1.000	0.	22.839	11.311	.2611E-03
11.439	1.053	.8365E-05	23.139	14.877	.3343E-03
11.739	1.106	.1597E-04	23.439	15.251	.3266E-03
12.039	1.148	.2151E-04	23.739	16.181	.3309E-03
12.339	1.197	.2761E-04	24.039	18.785	.3688E-03
12.639	1.210	.2845E-04	24.339	20.794	.3905E-03
12.939	1.214	.2792E-04	24.639	23.402	.4206E-03
13.239	1.220	.2757E-04	24.939	25.980	.4463E-03
13.539	1.237	.2860E-04	25.239	30.539	.5022E-03
13.839	1.239	.2772E-04	25.539	33.968	.5333E-03
14.139	1.226	.2525E-04	25.839	33.274	.4968E-03
14.439	1.113	.1199E-04	26.139	34.430	.4897E-03
14.739	1.096	.9733E-05	26.439	33.067	.4470E-03
15.039	1.074	.7178E-05	26.739	27.274	.3487E-03
15.339	1.059	.5422E-05	27.039	21.567	.2613E-03
15.639	1.055	.4840E-05	27.339	17.981	.2065E-03
15.939	1.083	.6878E-05	27.639	14.789	.1605E-03
16.239	1.104	.8259E-05	27.939	12.800	.1315E-03
16.539	1.169	.1276E-04	28.239	10.388	.1001E-03
16.839	1.240	.1726E-04	28.539	8.768	.7930E-04
17.139	1.337	.2296E-04	28.839	6.259	.5139E-04
17.439	1.420	.2714E-04	29.139	4.394	.3175E-04
17.739	1.535	.3282E-04	29.439	3.360	.2113E-04
18.039	1.612	.3567E-04	29.739	4.269	.2802E-04
18.339	1.701	.3879E-04	30.039	4.165	.2596E-04
18.639	1.894	.4697E-04	30.339	3.947	.2314E-04
18.939	2.044	.5199E-04	30.639	3.154	.1619E-04
19.239	2.118	.5276E-04	30.939	1.879	.6322E-05
19.539	2.288	.5756E-04	31.239	2.518	.1045E-04
19.839	1.964	.4079E-04	31.539	2.294	.8532E-05
20.139	1.651	.2608E-04	31.764	1.862	.5497E-05

TABLE A8. LIDAR DATA TAKEN ON JULY 9, 1982, BEGINNING AT 22.0°N, 67.5°W AT GMT 0508

Altitude, km	Scattering ratio	Scattering function, $(km\text{-}sr)^{-1}$	Altitude, km	Scattering ratio	Scattering function, $(km\text{-}sr)^{-1}$
11.139	1.000	0.	22.839	11.700	.2710E-03
11.439	1.009	.1409E-05	23.139	12.516	.2774E-03
11.739	1.014	.2167E-05	23.439	15.244	.3264E-03
12.039	1.019	.2720E-05	23.739	16.197	.3313E-03
12.339	1.027	.3772E-05	24.039	18.790	.3689E-03
12.639	1.035	.4777E-05	24.339	23.015	.4344E-03
12.939	1.056	.7343E-05	24.639	28.012	.5071E-03
13.239	1.084	.1048E-04	24.939	33.886	.5875E-03
13.539	1.069	.8294E-05	25.239	40.620	.6736E-03
13.839	1.092	.1072E-04	25.539	42.445	.6705E-03
14.139	1.111	.1240E-04	25.839	45.546	.6857E-03
14.439	1.156	.1657E-04	26.139	43.223	.6185E-03
14.739	1.240	.2431E-04	26.439	44.883	.6117E-03
15.039	1.282	.2716E-04	26.739	35.157	.4533E-03
15.339	1.086	.7905E-05	27.039	22.217	.2696E-03
15.639	1.080	.6975E-05	27.339	17.775	.2040E-03
15.939	1.109	.9101E-05	27.639	12.782	.1371E-03
16.239	1.157	.1245E-04	27.939	11.453	.1165E-03
16.539	1.210	.1583E-04	28.239	11.783	.1150E-03
16.839	1.278	.1993E-04	28.539	8.698	.7859E-04
17.139	1.347	.2365E-04	28.839	8.002	.6843E-04
17.439	1.416	.2692E-04	29.139	6.621	.5258E-04
17.739	1.486	.2983E-04	29.439	6.037	.4510E-04
18.039	1.583	.3401E-04	29.739	5.479	.3839E-04
18.339	1.688	.3810E-04	30.039	4.406	.2794E-04
18.639	1.962	.5054E-04	30.339	3.444	.1919E-04
18.939	2.162	.5785E-04	30.639	3.456	.1846E-04
19.239	2.187	.5598E-04	30.939	2.752	.1261E-04
19.539	2.199	.5355E-04	31.239	2.358	.9354E-05
19.839	2.085	.4590E-04	31.539	2.303	.8593E-05
20.139	2.123	.4502E-04	31.764	2.091	.6960E-05
20.439	2.424	.5405E-04			
20.739	2.678	.6034E-04			
21.039	2.786	.6104E-04			
21.339	2.789	.5816E-04			
21.639	3.585	.7996E-04			
21.939	6.176	.1523E-03			
22.239	7.755	.1891E-03			
22.539	9.093	.2155E-03			

TABLE A9. LIDAR DATA TAKEN ON JULY 9, 1982, BEGINNING AT 20.0°N, 67.0°W AT GMT 0531

Altitude, km	Scattering ratio	Scattering function, $(km\text{-}sr)^{-1}$	Altitude, km	Scattering ratio	Scattering function, $(km\text{-}sr)^{-1}$
11.139	1.034	.5497E-05	22.839	12.109	.2813E-03
11.439	1.013	.1980E-05	23.139	12.072	.2667E-03
11.739	1.000	0.	23.439	12.540	.2644E-03
12.039	1.008	.1122E-05	23.739	22.249	.4632E-03
12.339	1.016	.2276E-05	24.039	23.376	.4640E-03
12.639	1.028	.3792E-05	24.339	25.188	.4772E-03
12.939	1.050	.6555E-05	24.639	23.273	.4182E-03
13.239	1.077	.9619E-05	24.939	22.004	.3753E-03
13.539	1.117	.1409E-04	25.239	24.879	.4060E-03
13.839	1.139	.1611E-04	25.539	33.315	.5228E-03
14.139	1.105	.1175E-04	25.839	34.791	.5202E-03
14.439	1.128	.1358E-04	26.139	33.735	.4795E-03
14.739	1.182	.1846E-04	26.439	28.954	.3897E-03
15.039	1.243	.2340E-04	26.739	27.612	.3532E-03
15.339	1.119	.1095E-04	27.039	24.073	.2931E-03
15.639	1.070	.6088E-05	27.339	15.665	.1783E-03
15.939	1.087	.7219E-05	27.639	11.964	.1276E-03
16.239	1.133	.1051E-04	27.939	10.827	.1095E-03
16.539	1.195	.1472E-04	28.239	10.285	.9903E-04
16.839	1.262	.1881E-04	28.539	9.729	.8912E-04
17.139	1.343	.2339E-04	28.839	8.504	.7334E-04
17.439	1.431	.2790E-04	29.139	7.672	.6242E-04
17.739	1.491	.3014E-04	29.439	6.559	.4977E-04
18.039	1.601	.3501E-04	29.739	5.644	.3981E-04
18.339	1.899	.4974E-04	30.039	4.217	.2639E-04
18.639	2.116	.5865E-04	30.339	3.569	.2018E-04
18.939	2.296	.6453E-04	30.639	3.058	.1547E-04
19.239	2.621	.7646E-04	30.939	2.536	.1106E-04
19.539	3.244	.1003E-03	31.239	2.218	.8392E-05
19.839	3.383	.1008E-03	31.539	2.080	.7122E-05
20.139	3.549	.1022E-03	31.764	1.732	.4670E-05
20.439	3.483	.9426E-04			
20.739	3.559	.9202E-04			
21.039	3.739	.9361E-04			
21.339	4.690	.1200E-03			
21.639	6.248	.1623E-03			
21.939	7.189	.1821E-03			
22.239	8.761	.2172E-03			
22.539	11.335	.2751E-03			

TABLE A10. LIDAR DATA TAKEN ON JULY 11, 1982, BEGINNING AT 17.5°N, 64.5°W AT GMT 0216

Altitude, km	Scattering ratio	Scattering function, $(km\text{-}sr)^{-1}$	Altitude, km	Scattering ratio	Scattering function, $(km\text{-}sr)^{-1}$
11.139	1.917	.1482E-03	22.839	17.170	.4113E-03
11.439	2.098	.1715E-03	23.139	19.585	.4500E-03
11.739	2.191	.1799E-03	23.439	25.073	.5549E-03
12.039	2.264	.1845E-03	23.739	30.183	.6403E-03
12.339	2.244	.1755E-03	24.039	35.160	.7136E-03
12.639	1.444	.6039E-04	24.339	40.176	.7777E-03
12.939	1.149	.1948E-04	24.639	44.916	.8285E-03
13.239	1.070	.8861E-05	24.939	43.502	.7620E-03
13.539	1.000	0.	25.239	43.049	.7164E-03
13.839	1.041	.4843E-05	25.539	41.943	.6629E-03
14.139	1.099	.1117E-04	25.839	47.030	.7083E-03
14.439	1.178	.1911E-04	26.139	49.046	.7025E-03
14.739	1.232	.2375E-04	26.439	46.572	.6333E-03
15.039	1.204	.1984E-04	26.739	41.765	.5388E-03
15.339	1.266	.2465E-04	27.039	29.842	.3644E-03
15.639	1.299	.2636E-04	27.339	29.893	.3490E-03
15.939	1.315	.2646E-04	27.639	23.397	.2587E-03
16.239	1.327	.2612E-04	27.939	23.250	.2457E-03
16.539	1.432	.3291E-04	28.239	18.411	.1838E-03
16.839	1.540	.3908E-04	28.539	14.153	.1327E-03
17.139	1.650	.4467E-04	28.839	11.554	.1018E-03
17.439	1.772	.5040E-04	29.139	8.608	.7018E-04
17.739	1.959	.5949E-04	29.439	9.007	.7062E-04
18.039	2.294	.7623E-04	29.739	7.135	.5173E-04
18.339	2.779	.9951E-04	30.039	5.630	.3732E-04
18.639	2.929	.1025E-03	30.339	5.366	.3365E-04
18.939	2.957	.9847E-04	30.639	4.817	.2812E-04
19.239	2.936	.9213E-04	30.939	4.793	.2672E-04
19.539	3.129	.9577E-04	31.239	4.274	.2205E-04
19.839	2.855	.7889E-04	31.539	4.438	.2210E-04
20.139	2.845	.7418E-04	31.839	4.436	.2106E-04
20.439	3.240	.8514E-04	32.139	3.645	.1546E-04
20.739	3.257	.8112E-04	32.439	2.218	.6789E-05
21.039	5.907	.1677E-03	32.739	1.662	.3516E-05
21.339	7.154	.2002E-03	33.039	1.216	.1092E-05
21.639	7.847	.2121E-03	33.339	1.344	.1664E-05
21.939	9.617	.2540E-03	33.564	1.125	.5818E-06
22.239	10.779	.2745E-03			
22.539	15.680	.3922E-03			

TABLE A11. LIDAR DATA TAKEN ON JULY 11, 1982, BEGINNING AT 16.5°N, 63.0°W AT GMT 0238

Altitude, km	Scattering ratio	Scattering function, $(km\text{-}sr)^{-1}$	Altitude, km	Scattering ratio	Scattering function, $(km\text{-}sr)^{-1}$
11.139	1.121	.1963E-04	22.839	16.286	.3888E-03
11.439	1.054	.8416E-05	23.139	19.146	.4394E-03
11.739	1.047	.7099E-05	23.439	20.318	.4453E-03
12.039	1.031	.4496E-05	23.739	24.231	.5097E-03
12.339	1.019	.2646E-05	24.039	28.099	.5661E-03
12.639	1.026	.3544E-05	24.339	30.972	.5950E-03
12.939	1.004	.4818E-06	24.639	33.354	.6104E-03
13.239	1.000	0.	24.939	35.769	.6234E-03
13.539	1.030	.3610E-05	25.239	38.006	.6305E-03
13.839	1.038	.4451E-05	25.539	41.289	.6523E-03
14.139	1.044	.4942E-05	25.839	49.665	.7488E-03
14.439	1.086	.9237E-05	26.139	44.925	.6423E-03
14.739	1.109	.1116E-04	26.439	40.943	.5551E-03
15.039	1.137	.1330E-04	26.739	31.096	.3977E-03
15.339	1.174	.1610E-04	27.039	27.140	.3303E-03
15.639	1.194	.1711E-04	27.339	25.719	.2986E-03
15.939	1.208	.1750E-04	27.639	21.267	.2341E-03
16.239	1.232	.1854E-04	27.939	16.306	.1690E-03
16.539	1.294	.2240E-04	28.239	14.043	.1377E-03
16.839	1.388	.2810E-04	28.539	8.531	.7600E-04
17.139	1.530	.3645E-04	28.839	8.240	.6986E-04
17.439	1.719	.4696E-04	29.139	8.029	.6484E-04
17.739	1.894	.5543E-04	29.439	8.126	.6285E-04
18.039	2.067	.6283E-04	29.739	5.172	.3517E-04
18.339	2.322	.7399E-04	30.039	5.051	.3266E-04
18.639	2.496	.7953E-04	30.339	5.336	.3341E-04
18.939	2.675	.8431E-04	30.639	4.768	.2776E-04
19.239	3.364	.1125E-03	30.939	4.079	.2169E-04
19.539	3.498	.1123E-03	31.239	3.663	.1794E-04
19.839	3.692	.1145E-03	31.539	3.384	.1533E-04
20.139	3.074	.8340E-04	31.839	3.179	.1335E-04
20.439	2.693	.6436E-04	32.139	2.742	.1018E-04
20.739	2.628	.5851E-04	32.439	1.551	.3073E-05
21.039	6.043	.1723E-03	32.739	1.554	.2944E-05
21.339	6.709	.1857E-03	33.039	1.338	.1715E-05
21.639	7.887	.2133E-03			
21.939	9.182	.2412E-03			
22.239	11.580	.2969E-03			
22.539	13.838	.3430E-03			

TABLE A12. LIDAR DATA TAKEN ON JULY 11, 1982, BEGINNING AT 15.8°N, 63.0°W AT GMT 0247

Altitude, km	Scattering ratio	Scattering function, $(km\text{-}sr)^{-1}$	Altitude, km	Scattering ratio	Scattering function, $(km\text{-}sr)^{-1}$
11.139	1.425	.6900E-04	22.839	15.836	.3747E-03
11.439	1.822	.1287E-03	23.139	21.968	.5044E-03
11.739	2.287	.1947E-03	23.439	21.541	.4707E-03
12.039	2.481	.2161E-03	23.739	22.750	.4747E-03
12.339	1.897	.1263E-03	24.039	28.213	.5657E-03
12.639	1.379	.5135E-04	24.339	29.747	.5683E-03
12.939	1.195	.2539E-04	24.639	34.148	.6231E-03
13.239	1.022	.2701E-05	24.939	37.229	.6475E-03
13.539	1.000	0.	25.239	37.962	.6281E-03
13.839	1.030	.3504E-05	25.539	46.713	.7386E-03
14.139	1.056	.6228E-05	25.839	51.111	.7698E-03
14.439	1.064	.6811E-05	26.139	44.862	.6407E-03
14.739	1.119	.1210E-04	26.439	38.120	.5155E-03
15.039	1.184	.1791E-04	26.739	20.751	.2609E-03
15.339	1.243	.2255E-04	27.039	26.261	.3190E-03
15.639	1.246	.2176E-04	27.339	24.761	.2869E-03
15.939	1.241	.2033E-04	27.639	20.923	.2300E-03
16.239	1.292	.2343E-04	27.939	17.988	.1875E-03
16.539	1.350	.2677E-04	28.239	15.361	.1515E-03
16.839	1.437	.3174E-04	28.539	9.323	.8397E-04
17.139	1.545	.3750E-04	28.839	7.806	.6565E-04
17.439	1.727	.4736E-04	29.139	7.412	.5914E-04
17.739	2.014	.6256E-04	29.439	7.645	.5859E-04
18.039	2.265	.7396E-04	29.739	6.294	.4463E-04
18.339	2.555	.8615E-04	30.039	5.574	.3687E-04
18.639	2.856	.9745E-04	30.339	5.682	.3608E-04
18.939	3.186	.1086E-03	30.639	4.881	.2859E-04
19.239	3.712	.1274E-03	30.939	4.372	.2376E-04
19.539	3.753	.1223E-03	31.239	4.074	.2070E-04

TABLE A13. LIDAR DATA TAKEN ON JULY 11, 1982, BEGINNING AT 13.0°N, 62.8°W AT GMT 0320

Altitude, km	Scattering ratio	Scattering function, $(km\text{-}sr)^{-1}$	Altitude, km	Scattering ratio	Scattering function, $(km\text{-}sr)^{-1}$
11.139	1.315	.5116E-04	22.989	22.901	.5398E-03
11.439	1.333	.5224E-04	23.289	23.519	.5287E-03
11.739	1.397	.6003E-04	23.589	24.487	.5252E-03
12.039	1.783	.1142E-03	23.889	26.931	.5524E-03
12.339	2.213	.1708E-03	24.189	30.416	.5964E-03
12.639	3.158	.2927E-03	24.489	28.750	.5349E-03
12.939	3.170	.2832E-03	24.789	29.340	.5194E-03
13.239	3.138	.2685E-03	25.089	34.983	.5922E-03
13.539	3.811	.3398E-03	25.389	39.813	.6431E-03
13.839	3.972	.3457E-03	25.689	45.133	.6953E-03
14.139	4.072	.3439E-03	25.989	45.337	.6641E-03
14.439	4.363	.3594E-03	26.289	32.605	.4501E-03
14.814	1.000	0.	26.589	24.979	.3247E-03
15.189	1.007	.6494E-06	26.889	19.470	.2386E-03
15.489	1.088	.7916E-05	27.189	17.306	.2014E-03
15.789	1.172	.1483E-04	27.489	14.632	.1609E-03
16.089	1.243	.1996E-04	27.789	13.356	.1395E-03
16.389	1.268	.2102E-04	28.089	13.199	.1317E-03
16.689	1.305	.2275E-04	28.389	11.385	.1072E-03
16.989	1.397	.2807E-04	28.689	11.186	.1005E-03
17.289	1.635	.4247E-04	28.989	9.293	.7821E-04
17.589	1.786	.4982E-04	29.289	8.008	.6320E-04
17.889	2.516	.9110E-04	29.589	7.036	.5204E-04
18.189	2.827	.1040E-03	29.889	6.820	.4797E-04
18.489	3.097	.1131E-03	30.189	6.213	.4108E-04
18.789	3.463	.1258E-03	30.489	5.107	.3094E-04
19.089	3.659	.1285E-03	30.789	4.504	.2524E-04
19.389	3.341	.1070E-03	31.089	3.704	.1863E-04
19.689	3.634	.1138E-03	31.314	3.583	.1720E-04
19.989	4.694	.1509E-03			
20.289	5.325	.1671E-03			
20.589	5.502	.1645E-03			
20.889	5.659	.1684E-03			
21.189	6.194	.1714E-03			
21.489	10.059	.2848E-03			
21.789	10.533	.2855E-03			
22.089	12.071	.3158E-03			
22.389	16.332	.4165E-03			
22.689	19.756	.4854E-03			

TABLE A14. LIDAR DATA TAKEN ON JULY 12, 1982, BEGINNING AT 21.3°N, 66.8°W AT GMT 0016

Altitude, km	Scattering ratio	Scattering function, $(km\text{-}sr)^{-1}$	Altitude, km	Scattering ratio	Scattering function, $(km\text{-}sr)^{-1}$
10.835	1.037	.6243E-05	22.535	10.160	.2424E-03
11.135	1.034	.5558E-05	22.835	11.818	.2726E-03
11.435	1.023	.3600E-05	23.135	19.179	.4362E-03
11.735	1.008	.1169E-05	23.435	22.865	.4995E-03
12.035	1.000	0.	23.735	26.723	.5596E-03
12.335	1.008	.1184E-05	24.035	30.961	.6207E-03
12.635	1.054	.7261E-05	24.335	31.647	.6052E-03
12.935	1.110	.1438E-04	24.635	30.014	.5462E-03
13.235	1.142	.1790E-04	24.935	31.171	.5416E-03
13.535	1.141	.1710E-04	25.235	33.798	.5613E-03
13.835	1.339	.3960E-04	25.535	35.728	.5667E-03
14.135	1.646	.7268E-04	25.835	42.415	.6443E-03
14.435	1.980	.1052E-03	26.135	45.268	.6567E-03
14.735	1.186	.1900E-04	26.435	46.115	.6381E-03
15.035	1.151	.1467E-04	26.735	41.390	.5446E-03
15.335	1.227	.2103E-04	27.035	40.366	.5066E-03
15.635	1.211	.1860E-04	27.335	38.355	.4588E-03
15.935	1.127	.1063E-04	27.635	32.415	.3683E-03
16.235	1.172	.1374E-04	27.935	20.835	.2220E-03
16.535	1.211	.1601E-04	28.235	16.656	.1672E-03
16.835	1.249	.1789E-04	28.535	6.949	.6065E-04
17.135	1.318	.2169E-04	28.835	6.185	.5045E-04
17.435	1.425	.2743E-04	29.135	4.159	.2934E-04
17.735	1.491	.3005E-04	29.435	3.972	.2635E-04
18.035	1.718	.4160E-04	29.735	3.265	.1916E-04
18.335	2.147	.6301E-04	30.035	3.023	.1634E-04
18.635	2.412	.7344E-04	30.335	2.857	.1431E-04
18.935	2.305	.6430E-04	30.635	2.656	.1219E-04
19.235	2.273	.5942E-04	30.935	2.713	.1203E-04
19.535	2.283	.5669E-04	31.235	2.282	.8594E-05
19.835	2.281	.5361E-04	31.535	2.375	.8802E-05
20.135	2.134	.4497E-04	31.835	3.056	.1260E-04
20.435	2.150	.4317E-04	32.135	3.164	.1269E-04
20.735	4.122	.1110E-03	32.435	2.739	.9758E-05
21.035	3.732	.9234E-04	32.735	2.172	.6294E-05
21.335	5.928	.1586E-03	33.035	1.611	.3137E-05
21.635	7.500	.1992E-03	33.335	1.457	.2247E-05
21.935	7.983	.2038E-03	33.635	1.650	.3058E-05
22.235	8.252	.2015E-03	33.860	1.313	.1427E-05

TABLE A15. LIDAR DATA TAKEN ON JULY 12, 1982, BEGINNING AT 23.2°N, 67.4°W AT GMT 0042

Altitude, km	Scattering ratio	Scattering function, $(km\text{-}sr)^{-1}$	Altitude, km	Scattering ratio	Scattering function, $(km\text{-}sr)^{-1}$
10.835	1.011	.1910E-05	22.535	11.455	.2787E-03
11.135	1.011	.1809E-05	22.835	13.194	.3095E-03
11.435	1.000	0.	23.135	13.557	.3035E-03
11.735	1.036	.5526E-05	23.435	17.320	.3756E-03
12.035	1.083	.1213E-04	23.735	19.067	.3960E-03
12.335	1.090	.1272E-04	24.035	19.478	.3856E-03
12.635	1.068	.9270E-05	24.335	21.180	.4014E-03
12.935	1.063	.8278E-05	24.635	38.270	.7069E-03
13.235	1.083	.1052E-04	24.935	40.753	.7189E-03
13.535	1.162	.1984E-04	25.235	42.708	.7191E-03
13.835	1.231	.2717E-04	25.535	36.514	.5838E-03
14.135	1.256	.2903E-04	25.835	39.371	.6014E-03
14.435	1.267	.2892E-04	26.135	43.910	.6412E-03
14.735	1.241	.2476E-04	26.435	47.020	.6557E-03
15.035	1.251	.2459E-04	26.735	45.821	.6089E-03
15.335	1.268	.2499E-04	27.035	40.593	.5133E-03
15.635	1.279	.2477E-04	27.335	34.324	.4124E-03
15.935	1.200	.1689E-04	27.635	24.508	.2777E-03
16.235	1.192	.1539E-04	27.935	14.721	.1547E-03
16.535	1.236	.1806E-04	28.235	10.981	.1074E-03
16.835	1.295	.2138E-04	28.535	6.888	.6047E-04
17.135	1.331	.2270E-04	28.835	6.263	.5159E-04
17.435	1.582	.3785E-04	29.135	5.821	.4511E-04
17.735	1.623	.3837E-04	29.435	6.109	.4563E-04
18.035	1.815	.4759E-04	29.735	3.983	.2542E-04
18.335	2.009	.5580E-04	30.035	3.545	.2070E-04
18.635	2.240	.6499E-04	30.335	3.254	.1751E-04
18.935	2.292	.6414E-04	30.635	3.524	.1871E-04
19.235	2.252	.5887E-04	30.935	3.975	.2105E-04
19.535	2.315	.5854E-04	31.235	3.359	.1593E-04
19.835	2.153	.4862E-04	31.535	2.345	.8674E-05
20.135	2.000	.3992E-04	31.835	2.249	.7708E-05
20.435	2.075	.4065E-04	32.135	1.673	.3973E-05
20.735	2.595	.5712E-04	32.435	1.961	.5430E-05
21.035	2.793	.6105E-04	32.660	1.876	.4793E-05
21.335	3.011	.6519E-04			
21.635	3.044	.6309E-04			
21.935	9.422	.2476E-03			
22.235	10.753	.2730E-03			

TABLE A16. LIDAR DATA TAKEN ON JULY 12, 1982, BEGINNING AT 24.8°N, 68.0°W AT GMT 0102

Altitude, km	Scattering ratio	Scattering function, $(km\text{-}sr)^{-1}$	Altitude, km	Scattering ratio	Scattering function, $(km\text{-}sr)^{-1}$
10.835	.991	-.1574E-05	22.535	9.909	.2375E-03
11.135	1.019	.3044E-05	22.835	14.681	.3473E-03
11.435	1.023	.3651E-05	23.135	15.207	.3434E-03
11.735	1.002	.3005E-06	23.435	17.529	.3804E-03
12.035	1.000	0.	23.735	18.620	.3862E-03
12.335	1.027	.3779E-05	24.035	19.899	.3944E-03
12.635	1.048	.6556E-05	24.335	25.264	.4827E-03
12.935	1.057	.7543E-05	24.635	27.627	.5050E-03
13.235	1.136	.1724E-04	24.935	29.200	.5100E-03
13.535	1.229	.2799E-04	25.235	32.801	.5483E-03
13.835	1.327	.3848E-04	25.535	34.877	.5569E-03
14.135	1.379	.4301E-04	25.835	39.488	.6033E-03
14.435	1.371	.4010E-04	26.135	39.014	.5681E-03
14.735	1.367	.3779E-04	26.435	35.549	.4923E-03
15.035	1.327	.3202E-04	26.735	29.231	.3835E-03
15.335	1.267	.2492E-04	27.035	26.236	.3272E-03
15.635	1.194	.1722E-04	27.335	24.045	.2852E-03
15.935	1.215	.1814E-04	27.635	21.306	.2398E-03
16.235	1.239	.1916E-04	27.935	15.322	.1615E-03
16.535	1.285	.2179E-04	28.235	11.623	.1143E-03
16.835	1.344	.2497E-04	28.535	8.400	.7600E-04
17.135	1.390	.2676E-04	28.835	5.112	.4031E-04
17.435	1.488	.3175E-04	29.135	3.829	.2647E-04
17.735	1.779	.4800E-04	29.435	4.704	.3308E-04
18.035	1.808	.4716E-04	29.735	6.363	.4572E-04
18.335	1.955	.5284E-04	30.035	6.478	.4457E-04
18.635	2.364	.7147E-04	30.335	4.983	.3093E-04
18.935	2.484	.7366E-04	30.635	2.837	.1362E-04
19.235	2.408	.6620E-04	30.935	3.667	.1887E-04
19.535	2.184	.5271E-04	31.235	3.178	.1471E-04
19.835	2.087	.4585E-04	31.535	2.788	.1153E-04
20.135	1.978	.3907E-04	31.835	1.745	.4601E-05
20.435	1.987	.3733E-04	32.135	1.770	.4547E-05
20.735	2.408	.5045E-04	32.360	1.821	.4691E-05
21.035	3.211	.7527E-04			
21.335	3.436	.7898E-04			
21.635	3.415	.7457E-04			
21.935	3.011	.5913E-04			
22.235	3.944	.8242E-04			

TABLE A17. LIDAR DATA TAKEN ON JULY 12, 1982, BEGINNING AT 27.8°N, 68.8°W AT GMT 0143

Altitude, km	Scattering ratio	Scattering function, $(km\text{-}sr)^{-1}$	Altitude, km	Scattering ratio	Scattering function, $(km\text{-}sr)^{-1}$
10.835	1.083	.1391E-04	22.535	5.329	.1179E-03
11.135	1.088	.1422E-04	22.835	10.258	.2403E-03
11.435	1.076	.1186E-04	23.135	9.997	.2225E-03
11.735	1.030	.4473E-05	23.435	8.697	.1813E-03
12.035	1.005	.7994E-06	23.735	8.216	.1620E-03
12.335	1.021	.3009E-05	24.035	11.098	.2159E-03
12.635	1.000	0.	24.335	10.699	.1976E-03
12.935	1.017	.2167E-05	24.635	6.124	.9950E-04
13.235	1.057	.7177E-05	24.935	2.169	.2164E-04
13.535	1.103	.1249E-04	25.235	2.560	.2751E-04
13.835	1.156	.1819E-04	25.535	2.672	.2812E-04
14.135	1.207	.2314E-04	25.835	19.696	.2996E-03
14.435	1.235	.2509E-04	26.135	41.646	.6209E-03
14.735	1.279	.2827E-04	26.435	40.455	.5745E-03
15.035	1.356	.3419E-04	26.735	34.924	.4708E-03
15.335	1.426	.3889E-04	27.035	31.951	.4095E-03
15.635	1.486	.4212E-04	27.335	30.625	.3740E-03
15.935	1.317	.2606E-04	27.635	25.461	.2947E-03
16.235	1.290	.2266E-04	27.935	19.453	.2122E-03
16.535	1.256	.1899E-04	28.235	11.993	.1206E-03
16.835	1.310	.2188E-04	28.535	9.720	.9133E-04
17.135	1.411	.2757E-04	28.835	6.789	.5787E-04
17.435	1.445	.2835E-04	29.135	6.873	.5603E-04
17.735	1.734	.4442E-04	29.435	6.867	.5342E-04
18.035	1.881	.5069E-04	29.735	3.594	.2254E-04
18.335	1.930	.5088E-04	30.035	3.577	.2137E-04
18.635	2.051	.5465E-04	30.335	2.739	.1376E-04
18.935	2.281	.6331E-04	30.635	2.309	.9885E-05
19.235	2.294	.6081E-04	30.935	2.188	.8564E-05
19.535	2.186	.5300E-04	31.235	1.771	.5303E-05
19.835	1.858	.3645E-04	31.535	1.704	.4619E-05
20.135	1.695	.2806E-04			
20.435	1.834	.3203E-04			
20.735	2.007	.3676E-04			
21.035	2.359	.4718E-04			
21.335	2.827	.6041E-04			
21.635	3.071	.6526E-04			
21.935	3.928	.8789E-04			
22.235	3.424	.6932E-04			

TABLE A18. LIDAR DATA TAKEN ON JULY 12, 1982, BEGINNING AT 29.0°N, 69.2°W AT GMT 0158

Altitude, km	Scattering ratio	Scattering function, $(km\text{-}sr)^{-1}$	Altitude, km	Scattering ratio	Scattering function, $(km\text{-}sr)^{-1}$
10.835	1.218	.3677E-04	22.535	6.238	.1438E-03
11.135	1.220	.3573E-04	22.835	5.652	.1216E-03
11.435	1.187	.2940E-04	23.135	9.557	.2132E-03
11.735	1.034	.5230E-05	23.435	7.313	.1498E-03
12.035	1.000	0.	23.735	8.012	.1585E-03
12.335	1.004	.5652E-06	24.035	8.011	.1510E-03
12.635	1.025	.3364E-05	24.335	3.037	.4181E-04
12.935	1.163	.2144E-04	24.635	1.968	.1894E-04
13.235	1.458	.5793E-04	24.935	5.220	.7868E-04
13.535	1.131	.1598E-04	25.235	5.145	.7366E-04
13.835	1.212	.2480E-04	25.535	14.398	.2270E-03
14.135	1.269	.3033E-04	25.835	9.341	.1347E-03
14.435	1.318	.3418E-04	26.210	14.398	.2037E-03
14.735	1.392	.3995E-04	26.585	28.256	.3903E-03
15.035	1.446	.4321E-04	26.885	35.153	.4662E-03
15.335	1.519	.4772E-04	27.185	21.383	.2654E-03
15.635	1.595	.5196E-04	27.485	25.225	.3010E-03
15.935	1.709	.5876E-04	27.785	21.571	.2439E-03
16.235	1.542	.4268E-04	28.085	15.352	.1624E-03
16.535	1.503	.3760E-04	28.385	10.803	.1059E-03
16.835	1.448	.3180E-04	28.685	6.348	.5512E-04
17.135	1.500	.3373E-04	28.985	5.641	.4565E-04
17.435	1.587	.3767E-04	29.285	4.246	.3047E-04
17.735	1.663	.4044E-04	29.585	4.685	.3302E-04
18.035	1.927	.5376E-04	29.885	3.903	.2482E-04
18.335	2.039	.5727E-04	30.185	2.942	.1585E-04
18.635	2.090	.5710E-04	30.485	2.590	.1238E-04
18.935	2.343	.6688E-04	30.785	2.410	.1048E-04
19.235	2.389	.6574E-04	31.085	2.328	.9421E-05
19.535	2.139	.5126E-04	31.385	2.074	.7274E-05
19.835	1.980	.4192E-04	31.685	1.827	.5344E-05

TABLE A19. LIDAR DATA TAKEN ON JULY 12, 1982, BEGINNING AT 29.3°N, 69.3°W AT GMT 0202

Altitude, km	Scattering ratio	Scattering function, $(km\text{-}sr)^{-1}$	Altitude, km	Scattering ratio	Scattering function, $(km\text{-}sr)^{-1}$
10.835	1.145	.2432E-04	22.535	4.369	.9179E-04
11.135	1.174	.2807E-04	22.835	3.339	.6071E-04
11.435	1.058	.9042E-05	23.135	5.313	.1066E-03
11.735	1.019	.2890E-05	23.435	4.238	.7629E-04
12.035	1.002	.3341E-06	23.735	5.175	.9371E-04
12.335	1.000	0.	24.035	4.936	.8417E-04
12.635	1.014	.1831E-05	24.335	2.308	.2664E-04
12.935	1.033	.4247E-05	24.635	2.602	.3111E-04
13.235	1.034	.4232E-05	24.935	6.527	.1023E-03
13.535	1.074	.8925E-05	25.235	4.269	.5766E-04
13.835	1.208	.2422E-04	25.535	18.877	.3006E-03
14.135	1.269	.3005E-04	25.835	11.186	.1632E-03
14.435	1.305	.3252E-04	26.135	3.885	.4407E-04
14.735	1.357	.3616E-04	26.435	13.989	.1891E-03
15.035	1.416	.4002E-04	26.735	19.287	.2538E-03
15.335	1.488	.4452E-04	27.035	26.324	.3350E-03
15.635	1.552	.4785E-04	27.335	15.187	.1791E-03
15.935	1.673	.5540E-04	27.635	17.830	.2028E-03
16.235	1.549	.4288E-04	27.935	14.694	.1575E-03
16.535	1.534	.3960E-04	28.235	10.368	.1028E-03
16.835	1.451	.3180E-04	28.535	8.337	.7685E-04
17.135	1.493	.3300E-04	28.835	5.083	.4081E-04
17.435	1.541	.3447E-04	29.135	4.952	.3770E-04
17.735	1.598	.3623E-04	29.435	3.869	.2612E-04
18.035	1.924	.5316E-04	29.735	3.958	.2570E-04
18.335	1.972	.5316E-04	30.035	2.998	.1657E-04
18.635	2.017	.5289E-04	30.335	2.835	.1452E-04
18.935	2.111	.5493E-04	30.635	2.586	.1198E-04
19.235	2.382	.6497E-04	30.935	2.348	.9716E-05
19.535	2.105	.4938E-04	31.235	2.228	.8449E-05
19.835	1.853	.3622E-04	31.535	2.026	.6736E-05
20.135	1.753	.3039E-04			
20.435	1.709	.2722E-04			
20.735	2.250	.4564E-04			
21.035	2.261	.4377E-04			
21.335	2.286	.4251E-04			
21.635	1.988	.3113E-04			
21.935	1.769	.2309E-04			
22.235	2.331	.3806E-04			

TABLE A20. LIDAR DATA TAKEN ON JULY 12, 1982, BEGINNING AT 29.5°N, 69.3°W AT GMT 0205

Altitude, km	Scattering ratio	Scattering function, $(km\text{-}sr)^{-1}$	Altitude, km	Scattering ratio	Scattering function, $(km\text{-}sr)^{-1}$
10.835	1.206	.3447E-04	22.535	3.275	.6197E-04
11.135	1.084	.1362E-04	22.835	3.012	.5223E-04
11.435	1.040	.6186E-05	23.135	3.096	.5183E-04
11.735	1.007	.1122E-05	23.435	3.609	.6147E-04
12.035	1.020	.2882E-05	23.735	3.764	.6204E-04
12.335	1.008	.1064E-05	24.035	3.057	.4398E-04
12.635	1.000	0.	24.335	2.312	.2674E-04
12.935	1.025	.3266E-05	24.635	2.362	.2645E-04
13.235	1.041	.5084E-05	24.935	5.490	.8310E-04
13.535	1.040	.4845E-05	25.235	3.479	.4373E-04
13.835	1.157	.1825E-04	25.535	14.603	.2287E-03
14.135	1.200	.2232E-04	25.835	8.695	.1233E-03
14.435	1.285	.3040E-04	26.135	2.850	.2826E-04
14.735	1.321	.3245E-04	26.435	8.430	.1082E-03
15.035	1.345	.3314E-04	26.735	13.775	.1773E-03
15.335	1.451	.4115E-04	27.035	9.729	.1155E-03
15.635	1.564	.4888E-04	27.335	2.965	.2481E-04
15.935	1.639	.5260E-04	27.635	11.955	.1320E-03
16.235	1.579	.4526E-04	27.935	7.148	.7070E-04
16.535	1.609	.4520E-04	28.235	6.340	.5860E-04
16.835	1.394	.2779E-04	28.535	9.232	.8622E-04
17.135	1.460	.3084E-04	28.835	6.534	.5532E-04
17.435	1.521	.3317E-04	29.135	4.684	.3514E-04
17.735	1.601	.3638E-04	29.435	3.219	.2020E-04
18.035	1.826	.4756E-04	29.735	3.504	.2176E-04
18.335	1.995	.5445E-04	30.035	3.250	.1866E-04
18.635	1.974	.5063E-04	30.335	2.716	.1358E-04
18.935	2.125	.5561E-04	30.635	2.662	.1255E-04
19.235	2.284	.6034E-04	30.935	2.147	.8265E-05
19.535	2.142	.5102E-04	31.235	2.403	.9653E-05
19.835	1.805	.3419E-04	31.535	1.756	.4962E-05
20.135	1.789	.3186E-04			
20.435	1.726	.2789E-04			
20.735	2.189	.4339E-04			
21.035	2.262	.4382E-04			
21.335	2.337	.4421E-04			
21.635	1.652	.2055E-04			
21.935	1.486	.1460E-04			
22.235	1.329	.9419E-05			

TABLE A21. LIDAR DATA TAKEN ON JULY 12, 1982, BEGINNING AT 30.2°N, 69.6°W AT GMT 0213

Altitude, km	Scattering ratio	Scattering function, $(km\text{-}sr)^{-1}$	Altitude, km	Scattering ratio	Scattering function, $(km\text{-}sr)^{-1}$
10.835	1.322	.5430E-04	22.535	1.593	.1627E-04
11.135	1.430	.7003E-04	22.835	2.147	.2998E-04
11.435	1.544	.8550E-04	23.135	2.950	.4858E-04
11.735	1.844	.1282E-03	23.435	3.469	.5859E-04
12.035	2.003	.1472E-03	23.735	3.895	.6546E-04
12.335	2.322	.1874E-03	24.035	3.889	.6223E-04
12.635	3.224	.3037E-03	24.335	3.419	.4965E-04
12.935	3.294	.3015E-03	24.635	2.614	.3157E-04
13.235	1.223	.2814E-04	24.935	3.717	.5065E-04
13.535	1.170	.2074E-04	25.235	2.494	.2654E-04
13.835	1.224	.2627E-04	25.535	2.139	.1929E-04
14.135	1.296	.3336E-04	25.835	1.352	.5677E-05
14.435	1.333	.3580E-04	26.135	1.233	.3585E-05
14.735	1.216	.2202E-04	26.435	1.530	.7781E-05
15.035	1.336	.3251E-04	26.735	1.000	0.
15.335	1.470	.4325E-04	27.035	1.089	.1183E-05
15.635	1.590	.5153E-04	27.335	1.267	.3392E-05
15.935	1.785	.6506E-04	27.635	4.321	.4031E-04
16.235	1.849	.6685E-04	27.935	5.787	.5546E-04
16.535	1.954	.7132E-04	28.235	2.601	.1770E-04
16.835	1.971	.6895E-04	28.535	3.967	.3131E-04
17.135	1.608	.4101E-04	28.835	2.078	.1085E-04
17.435	1.692	.4439E-04	29.135	4.269	.3142E-04
17.735	1.999	.6096E-04	29.435	4.230	.2963E-04
18.035	2.108	.6422E-04	29.735	2.608	.1408E-04
18.335	2.216	.6704E-04	30.035	3.681	.2239E-04
18.635	2.288	.6747E-04	30.335	3.118	.1689E-04
18.935	2.269	.6317E-04	30.635	2.778	.1353E-04
19.235	2.391	.6584E-04	30.935	2.247	.9052E-05
19.535	2.444	.6500E-04	31.235	1.957	.6634E-05
19.835	1.934	.3996E-04	31.535	1.298	.1972E-05
20.135	2.014	.4127E-04	31.760	1.232	.1434E-05

TABLE A22. LIDAR DATA TAKEN ON JULY 12, 1982, BEGINNING AT 32.3°N, 70.1°W AT GMT 0238

Altitude, km	Scattering ratio	Scattering function, $(km\text{-}sr)^{-1}$	Altitude, km	Scattering ratio	Scattering function, $(km\text{-}sr)^{-1}$
12.054	1.263	.3857E-04	23.754	4.014	.6794E-04
12.354	1.464	.6560E-04	24.054	5.258	.9144E-04
12.654	1.900	.1227E-03	24.354	4.793	.7761E-04
12.954	2.412	.1851E-03	24.654	3.599	.5069E-04
13.254	2.651	.2083E-03	24.954	2.341	.2493E-04
13.554	2.220	.1480E-03	25.254	2.054	.1868E-04
13.854	1.735	.8585E-04	25.554	1.541	.9131E-05
14.154	1.300	.3373E-04	25.854	1.368	.5917E-05
14.454	1.465	.4978E-04	26.154	1.286	.4389E-05
14.754	1.569	.5781E-04	26.454	1.119	.1734E-05
15.054	1.510	.4919E-04	26.754	1.011	.1497E-06
15.354	1.495	.4537E-04	27.054	1.022	.2965E-06
15.654	1.464	.4036E-04	27.354	1.000	0.
15.954	1.554	.4581E-04	27.654	1.019	.2267E-06
16.254	1.667	.5235E-04	27.954	1.012	.1401E-06
16.554	2.039	.7737E-04	28.254	.948	-.5769E-06
16.854	2.164	.8242E-04	28.554	1.030	.3131E-06
17.154	2.191	.8011E-04	28.854	.935	-.6525E-06
17.454	2.031	.6596E-04	29.154	1.086	.8264E-06
17.754	1.971	.5900E-04	29.454	1.019	.1715E-06
18.054	2.120	.6470E-04	29.754	.977	-.2000E-06
18.354	2.284	.7052E-04	30.054	1.248	.2062E-05
18.654	2.386	.7239E-04	30.354	1.415	.3295E-05
18.954	2.183	.5871E-04	30.654	1.859	.6520E-05
19.254	2.447	.6828E-04	30.954	1.898	.6502E-05
19.554	2.318	.5912E-04	31.254	1.457	.3157E-05
19.854	1.768	.3277E-04	31.554	1.323	.2127E-05
20.154	1.557	.2261E-04	31.779	1.442	.2729E-05
20.454	1.840	.3241E-04			
20.754	2.617	.5926E-04			
21.054	3.571	.8964E-04			
21.354	3.965	.9847E-04			
21.654	6.254	.1663E-03			
21.954	9.884	.2678E-03			
22.254	9.701	.2499E-03			
22.554	8.253	.1985E-03			
22.854	3.242	.5843E-04			
23.154	2.536	.3815E-04			
23.454	3.022	.4784E-04			

TABLE A23. LIDAR DATA TAKEN ON JULY 12, 1982, BEGINNING AT 34.2°N, 70.7°W AT GMT 0306

Altitude, km	Scattering ratio	Scattering function, $(km\text{-}sr)^{-1}$	Altitude, km	Scattering ratio	Scattering function, $(km\text{-}sr)^{-1}$
12.054	1.569	.8327E-04	23.754	1.523	.1178E-04
12.354	1.487	.6882E-04	24.054	1.301	.6474E-05
12.654	1.487	.6629E-04	24.354	1.146	.2983E-05
12.954	1.417	.5469E-04	24.654	1.069	.1340E-05
13.254	1.467	.5893E-04	24.954	1.067	.1239E-05
13.554	1.578	.7014E-04	25.254	1.000	0.
13.854	1.674	.7867E-04	25.554	1.033	.5535E-06
14.154	1.295	.3321E-04	25.854	1.016	.2589E-06
14.454	1.140	.1497E-04	26.154	1.024	.3757E-06
14.754	1.231	.2345E-04	26.454	1.012	.1759E-06
15.054	1.376	.3632E-04	26.754	1.049	.6851E-06
15.354	1.685	.6279E-04	27.054	1.080	.1068E-05
15.654	1.536	.4661E-04	27.354	1.081	.1029E-05
15.954	1.551	.4556E-04	27.654	1.090	.1091E-05
16.254	1.769	.6031E-04	27.954	1.025	.2921E-06
16.554	1.842	.6271E-04	28.254	1.057	.6309E-06
16.854	2.280	.9058E-04	28.554	1.066	.6923E-06
17.154	2.382	.9301E-04	28.854	.956	-.4394E-06
17.454	2.412	.9032E-04	29.154	1.033	.3129E-06
17.754	2.442	.8765E-04	29.454	1.014	.1259E-06
18.054	2.269	.7332E-04	29.754	1.127	.1110E-05
18.354	2.338	.7348E-04	30.054	1.044	.3681E-06
18.654	2.463	.7639E-04	30.354	1.161	.1283E-05
18.954	2.402	.6960E-04	30.654	1.248	.1882E-05
19.254	2.193	.5628E-04	30.954	1.421	.3048E-05
19.554	2.152	.5167E-04	31.254	1.382	.2637E-05
19.854	1.530	.2260E-04	31.554	1.332	.2192E-05
20.154	1.434	.1762E-04	31.779	1.386	.2378E-05
20.454	1.410	.1581E-04			
20.754	1.464	.1701E-04			
21.054	1.582	.2028E-04			
21.354	3.987	.9919E-04			
21.654	4.126	.9890E-04			
21.954	10.484	.2859E-03			
22.254	14.737	.3945E-03			
22.554	15.473	.3960E-03			
22.854	8.165	.1868E-03			
23.154	4.728	.9258E-04			
23.454	1.505	.1195E-04			

TABLE A24. LIDAR DATA TAKEN ON JULY 12, 1982, BEGINNING AT 38.5°N, 72.0°W AT GMT 0403

Altitude, km	Scattering ratio	Scattering function, $(km\text{-}sr)^{-1}$	Altitude, km	Scattering ratio	Scattering function, $(km\text{-}sr)^{-1}$
12.054	1.257	.3760E-04	23.754	1.123	.2807E-05
12.354	1.293	.4133E-04	24.054	1.113	.2471E-05
12.654	1.308	.4166E-04	24.354	1.072	.1496E-05
12.954	1.351	.4520E-04	24.654	1.059	.1179E-05
13.254	1.395	.4858E-04	24.954	1.043	.8101E-06
13.554	1.436	.5112E-04	25.254	1.012	.2129E-06
13.854	1.404	.4517E-04	25.554	1.046	.7956E-06
14.154	1.333	.3545E-04	25.854	1.047	.7618E-06
14.454	1.389	.3962E-04	26.154	1.039	.6046E-06
14.754	1.581	.5654E-04	26.454	1.021	.3132E-06
15.054	1.669	.6226E-04	26.754	1.019	.2721E-06
15.354	1.679	.6046E-04	27.054	1.056	.7467E-06
15.654	1.845	.7195E-04	27.354	1.142	.1824E-05
15.954	1.834	.6787E-04	27.654	1.004	.5042E-07
16.254	1.677	.5268E-04	27.954	1.000	0.
16.554	1.820	.6107E-04	28.254	1.069	.7701E-06
16.854	2.032	.7325E-04	28.554	1.087	.9214E-06
17.154	2.495	.1009E-03	28.854	1.095	.9645E-06
17.454	2.561	.1001E-03	29.154	1.008	.7318E-07
17.754	2.311	.7994E-04	29.454	.987	-.1225E-06
18.054	2.245	.7216E-04	29.754	1.019	.1694E-06
18.354	2.066	.5878E-04	30.054	1.171	.1429E-05
18.654	1.836	.4378E-04	30.354	1.099	.7929E-06
18.954	2.397	.6958E-04	30.654	1.106	.8035E-06
19.254	2.574	.7451E-04	30.954	1.240	.1738E-05
19.554	2.101	.4954E-04	31.254	1.146	.1010E-05
19.854	1.754	.3224E-04	31.554	1.073	.4813E-06
20.154	1.712	.2892E-04	31.779	1.084	.5156E-06
20.454	1.269	.1039E-04			
20.754	1.304	.1116E-04			
21.054	1.356	.1242E-04			
21.354	1.509	.1691E-04			
21.654	2.123	.3561E-04			
21.954	2.842	.5575E-04			
22.254	3.063	.5957E-04			
22.554	2.729	.4763E-04			
22.854	1.612	.1609E-04			
23.154	1.275	.6893E-05			
23.454	1.124	.2965E-05			

TABLE A25. LIDAR DATA TAKEN ON JULY 12, 1982, BEGINNING AT 42.0°N, 73.7°W AT GMT 0506

Altitude, km	Scattering ratio	Scattering function, $(km\text{-}sr)^{-1}$	Altitude, km	Scattering ratio	Scattering function, $(km\text{-}sr)^{-1}$
12.663	1.309	.4157E-04	24.363	1.106	.2212E-05
12.963	1.305	.3943E-04	24.663	1.000	0.
13.263	1.312	.3891E-04	24.963	1.021	.3928E-06
13.563	1.357	.4286E-04	25.263	1.156	.2806E-05
13.863	1.479	.5551E-04	25.563	1.105	.1803E-05
14.163	1.766	.8541E-04	25.863	1.059	.9588E-06
14.463	1.668	.7098E-04	26.163	1.004	.6491E-07
14.763	1.447	.4508E-04	26.463	1.111	.1644E-05
15.063	1.731	.6995E-04	26.763	1.059	.8309E-06
15.363	1.791	.7194E-04	27.063	1.070	.9392E-06
15.663	1.824	.7110E-04	27.363	1.119	.1523E-05
15.963	1.750	.6144E-04	27.663	1.079	.9671E-06
16.263	1.824	.6412E-04	27.963	1.063	.7340E-06
16.563	1.964	.7122E-04	28.263	1.037	.4150E-06
16.863	2.098	.7712E-04	28.563	1.030	.3226E-06
17.163	2.503	.1002E-03	28.863	1.017	.1709E-06
17.463	2.454	.9215E-04	29.163	1.055	.5301E-06
17.763	2.168	.7035E-04	29.463	1.102	.9428E-06
18.063	2.174	.6716E-04	29.763	1.035	.3135E-06
18.363	2.096	.5961E-04	30.063	1.055	.4649E-06
18.663	1.825	.4263E-04	30.363	1.115	.9283E-06
18.963	1.703	.3453E-04	30.663	1.069	.5332E-06
19.263	1.482	.2256E-04	30.963	1.096	.7061E-06
19.563	2.057	.4714E-04	31.263	1.183	.1284E-05
19.863	2.215	.5162E-04	31.563	1.116	.7795E-06
20.163	1.652	.2642E-04	31.863	1.153	.9292E-06
20.463	1.368	.1423E-04			
20.763	1.246	.9058E-05			
21.063	1.136	.4759E-05			
21.363	1.241	.8060E-05			
21.663	1.630	.2010E-04			
21.963	3.402	.7303E-04			
22.263	3.327	.6747E-04			
22.563	2.473	.4074E-04			
22.863	1.339	.8926E-05			
23.163	1.122	.3061E-05			
23.463	1.092	.2214E-05			
23.763	1.141	.3219E-05			
24.063	1.184	.4015E-05			

References

1. Labitzke, K.; Naujokat, B.; and McCormick, M. P.: Temperature Effects on the Stratosphere of the April 4, 1982 Eruption of El Chichon, Mexico. *Geophys. Res. Lett.*, vol. 10, no. 1, Jan. 1983, pp. 24–26.
2. Russell, Philip B.; Swissler, Thomas J.; and McCormick, M. Patrick: Methodology for Error Analysis and Simulation of Lidar Aerosol Measurements. *Appl. Opt.*, vol. 18, no. 22, Nov. 15, 1979, pp. 3783–3797.
3. McCormick, M. P.; Swissler, T. J.; Chu, W. P.; and Fuller, W. H., Jr.: Post-Volcanic Stratospheric Aerosol Decay as Measured by Lidar. *J. Atmos. Sci.*, vol. 35, no. 7, July 1978, pp. 1296–1303.
4. McCormick, M. P.; Trepte, C. R.; and Kent, G. S.: Spatial Changes in the Stratospheric Aerosol Associated With the North Polar Vortex. *Geophys. Res. Lett.*, vol. 10, no. 10, Oct. 1983, pp. 941–944.
5. Hofmann, D. J.; and Rosen, J. M.: Stratospheric Sulfuric Acid Fraction and Mass Estimate for the 1982 Volcanic Eruption of El Chichon. *Geophys. Res. Lett.*, vol. 10, no. 4, Apr. 1983, pp. 313–316.
6. McCormick, M. P.; Swissler, T. J.; Fuller, W. H.; Hunt, W. H.; and Osborn, M. T.: Airborne and Ground-Based Lidar Measurements of the El Chichon Stratospheric Aerosol From 90°N to 56°S. *Geofis. Int.*, vol. 23, no. 2, Apr. 1984, pp. 187–221.

Standard Bibliographic Page

1. Report No.	2. Government Accession No.	3. Recipient's Catalog No.
NASA RP-1166		

4. Title and Subtitle	5. Report Date
Airborne Lidar Measurements of El Chichon Stratospheric Aerosols—July 1982	July 1986
	6. Performing Organization Code: 672-21-14-70
7. Author(s): M. Patrick McCormick and M. T. Osborn	8. Performing Organization Report No.: L-16107
9. Performing Organization Name and Address: NASA Langley Research Center, Hampton, VA 23665-5225	10. Work Unit No.
	11. Contract or Grant No.
12. Sponsoring Agency Name and Address: National Aeronautics and Space Administration, Washington, DC 20546-0001	13. Type of Report and Period Covered: Reference Publication
	14. Sponsoring Agency Code

15. Supplementary Notes

M. Patrick McCormick: Langley Research Center, Hampton, Virginia.
M. T. Osborn: SASC Technologies, Inc., Hampton, Virginia.
Previous reports in this series: NASA RP-1136 and NASA RP-1148.

16. Abstract

A NASA Electra airplane outfitted with a lidar system was flown in July 1982 between the latitudes of 42°N and 12°N. The primary purpose of this mission was to determine the spatial distribution and aerosol characteristics of the El Chichon–produced stratospheric material. This report presents the lidar data from that flight mission. Representative profiles of lidar backscatter ratio, plots of the integrated backscattering function versus latitude, and contours of backscatter mixing ratio versus altitude and latitude are given. In addition, tables containing numerical values of the backscatter ratio and backscattering function versus altitude are supplied for each profile. The largest amount of material produced by the El Chichon eruptions of late March–early April 1982 which was measured by this flight resided south of 30°N and was concentrated above 21 km in a layer that peaked at 24 to 27 km. In this latitude region, peak backscatter ratios at a wavelength of 0.6943 μm were approximately 50, and peak optical depths were calculated to be 0.2. This report presents the results of this mission in a ready-to-use format for atmospheric and climatic studies.

17. Key Words (Suggested by Authors(s))	18. Distribution Statement
Lidar Volcanoes El Chichon Stratospheric aerosols	Unclassified—Unlimited Subject Category 46

19. Security Classif.(of this report)	20. Security Classif.(of this page)	21. No. of Pages	22. Price
Unclassified	Unclassified	49	A03

For sale by the National Technical Information Service, Springfield, Virginia 22161

NASA-Langley, 1986

National Aeronautics and
Space Administration
Code NIT-4

Washington, D.C.
20546-0001

Official Business
Penalty for Private Use, $300

BULK RATE
POSTAGE & FEES PAID
NASA
Permit No. G-27

POSTMASTER: If Undeliverable (Section 158
Postal Manual) Do Not Return